**LIPEI DU**
UC BERKELEY / LBNL

# THEORY OVERVIEW ON BEAM ENERGY SCAN

**2025 RHIC/AGS ANNUAL USERS' MEETING**
MAY 20, 2025

# QCD PHASE DIAGRAM



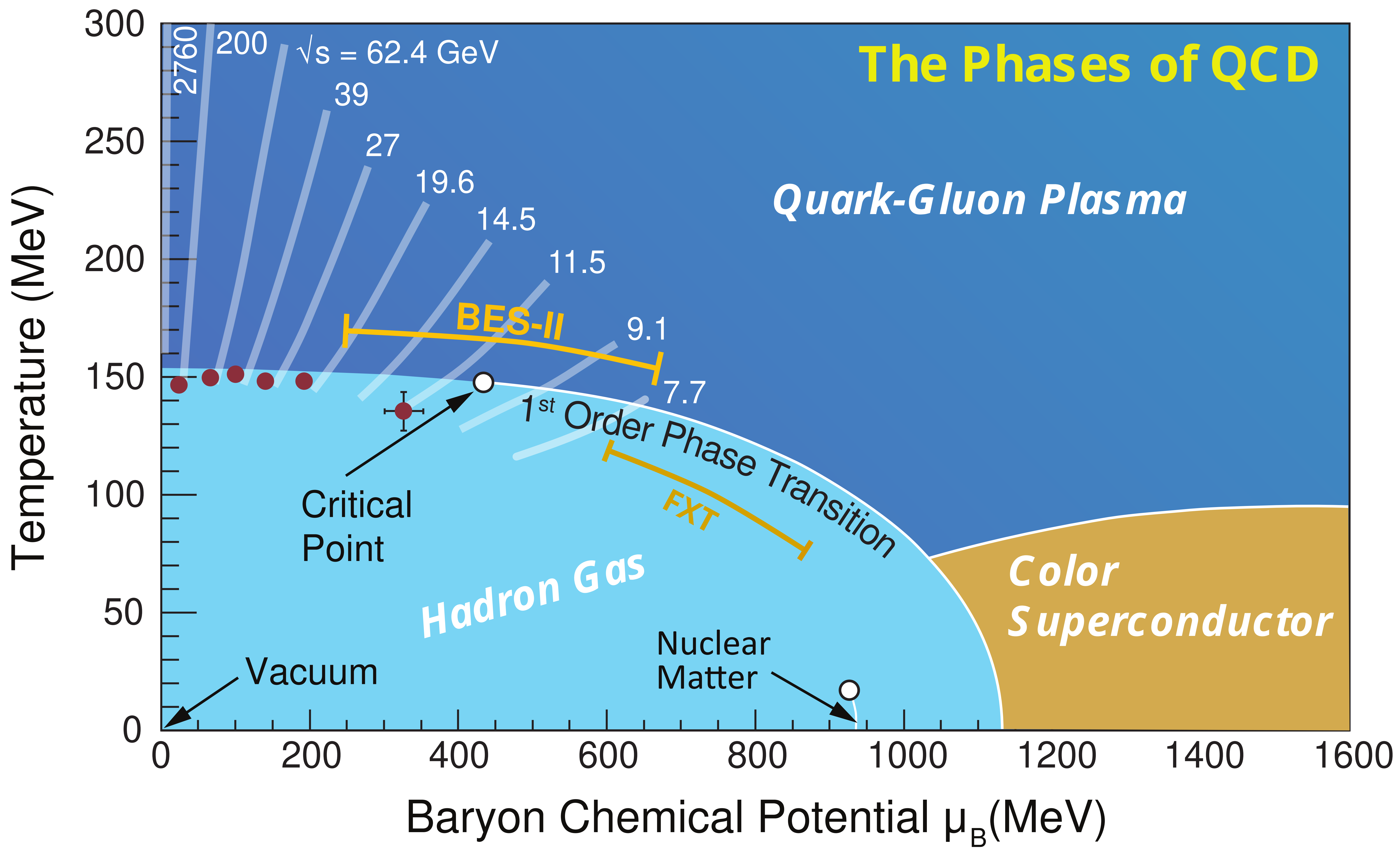


fig: Du, Sorensen, and Stephanov, 2402.10183, modified from Bzdak, Esumi, Koch, Liao, Stephanov, and Xu, Phys. Rept. 853 (2020)

# LONGITUDINAL DYNAMICS

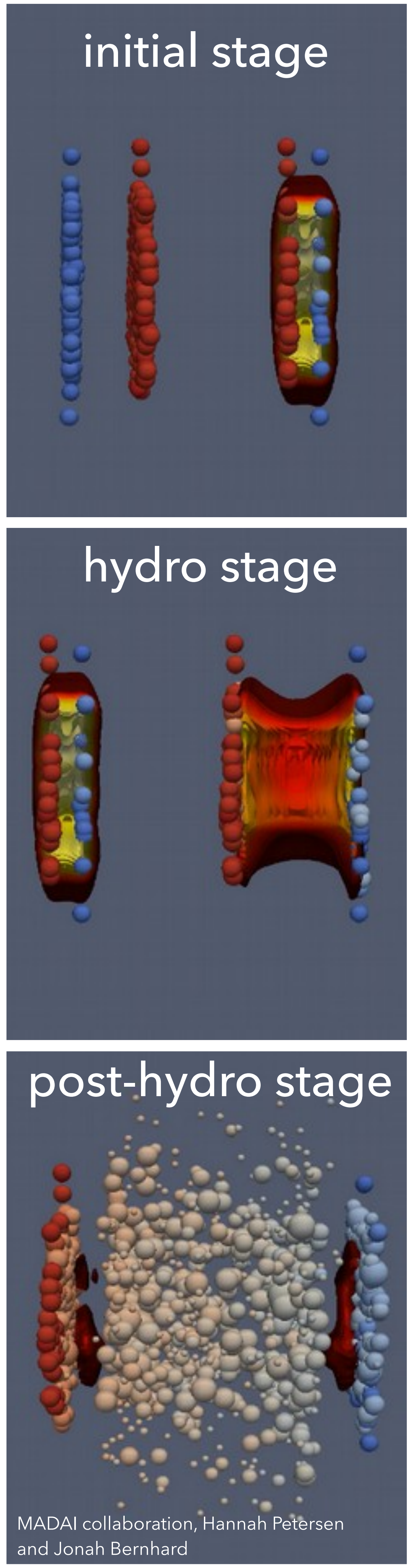


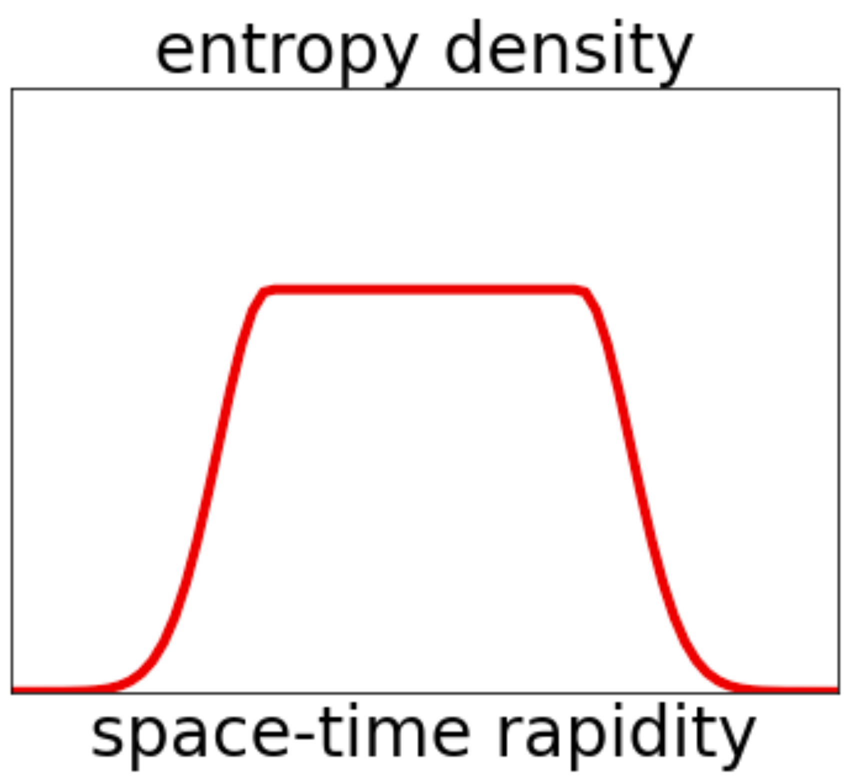


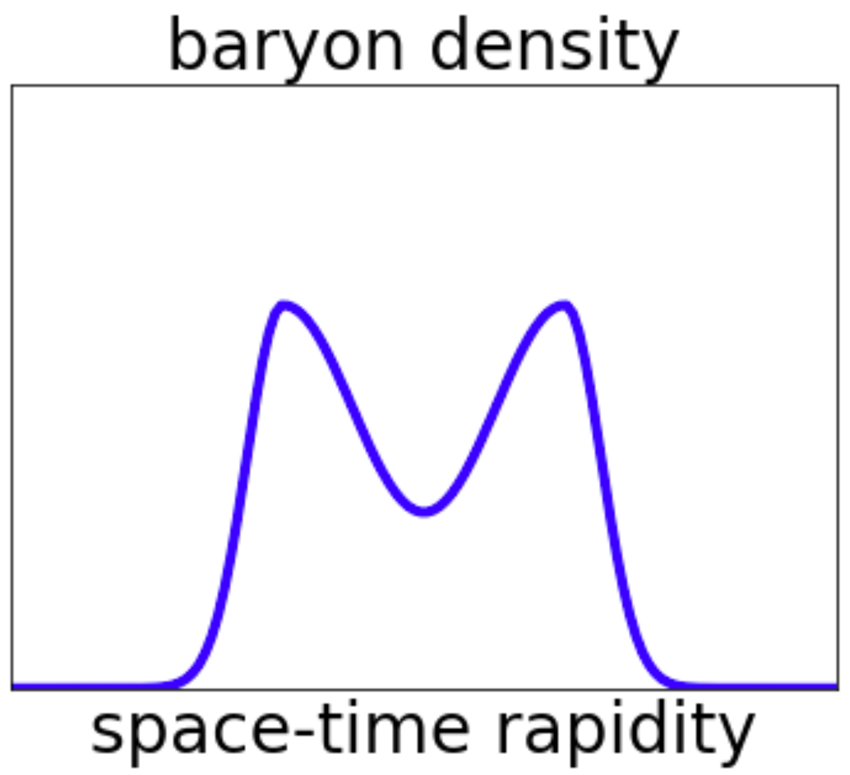


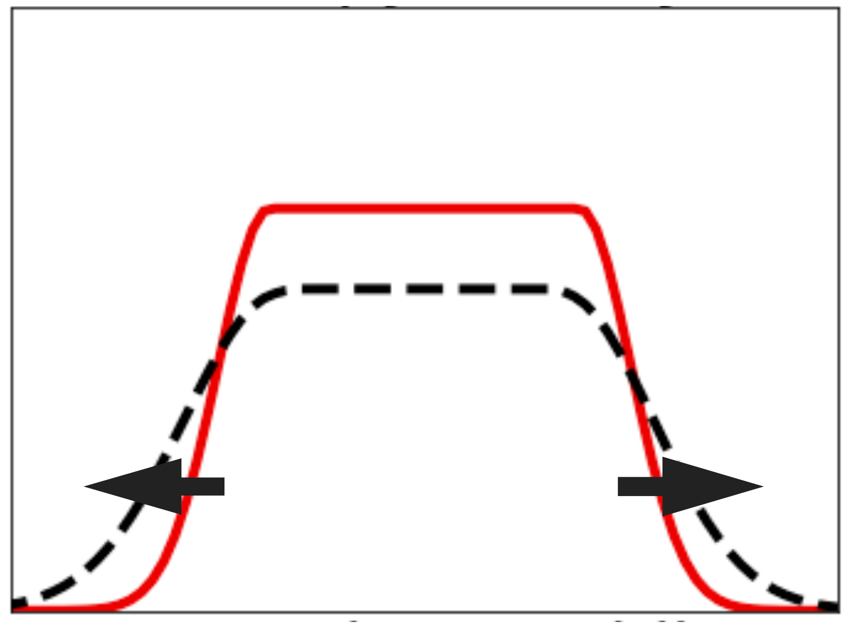

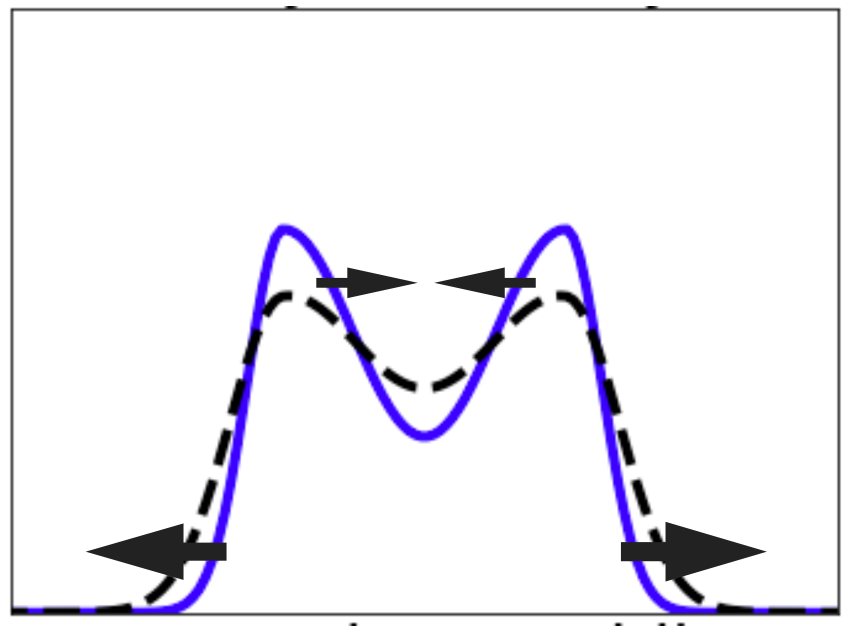

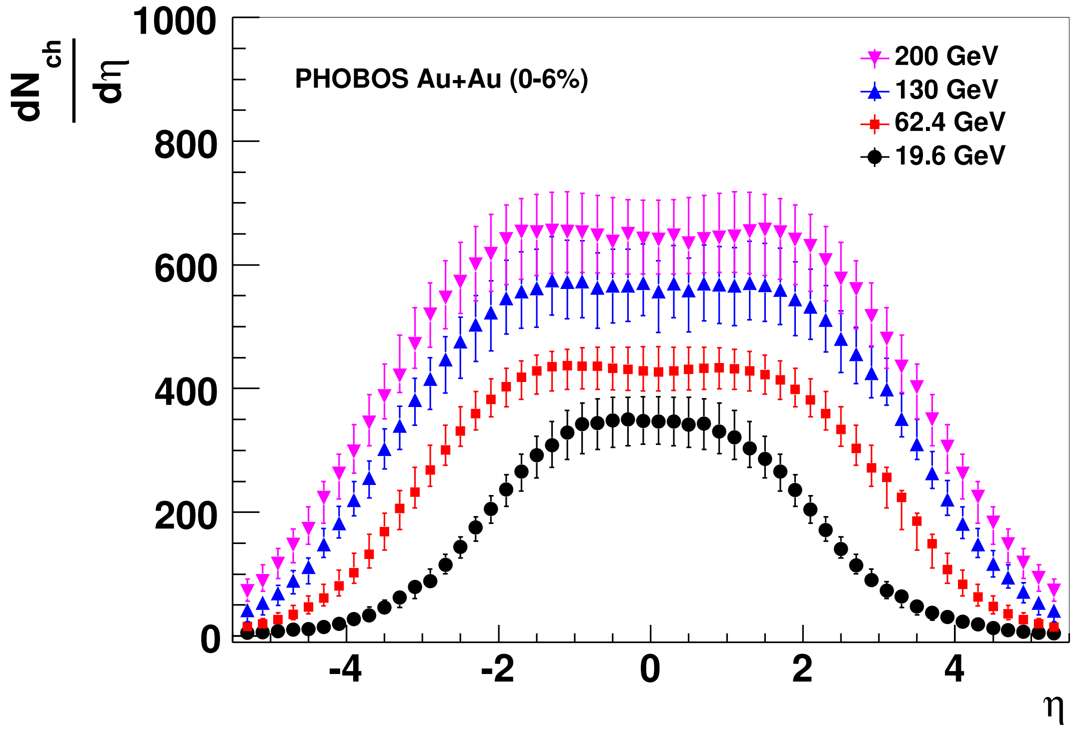


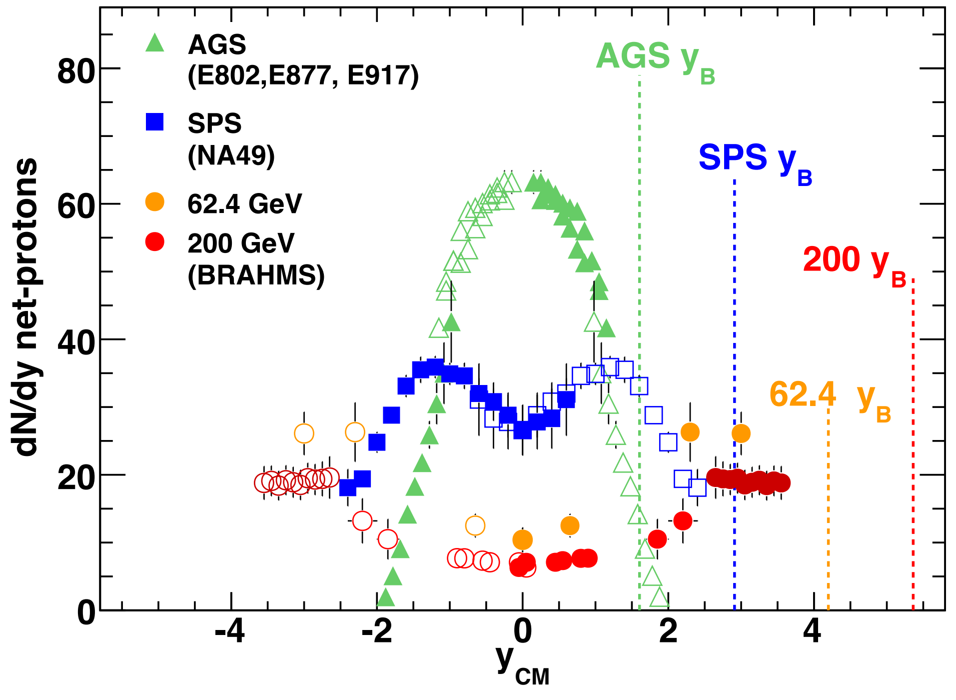


- initial energy deposition
- initial baryon stopping

+

- longitudinal pressure gradient ⟹ longitudinal flow & expansion
- baryon density gradient ⟹ baryon diffusion (hydro transport)

- rapidity-dependent particle distributions

# 3D INITIAL CONDITIONS



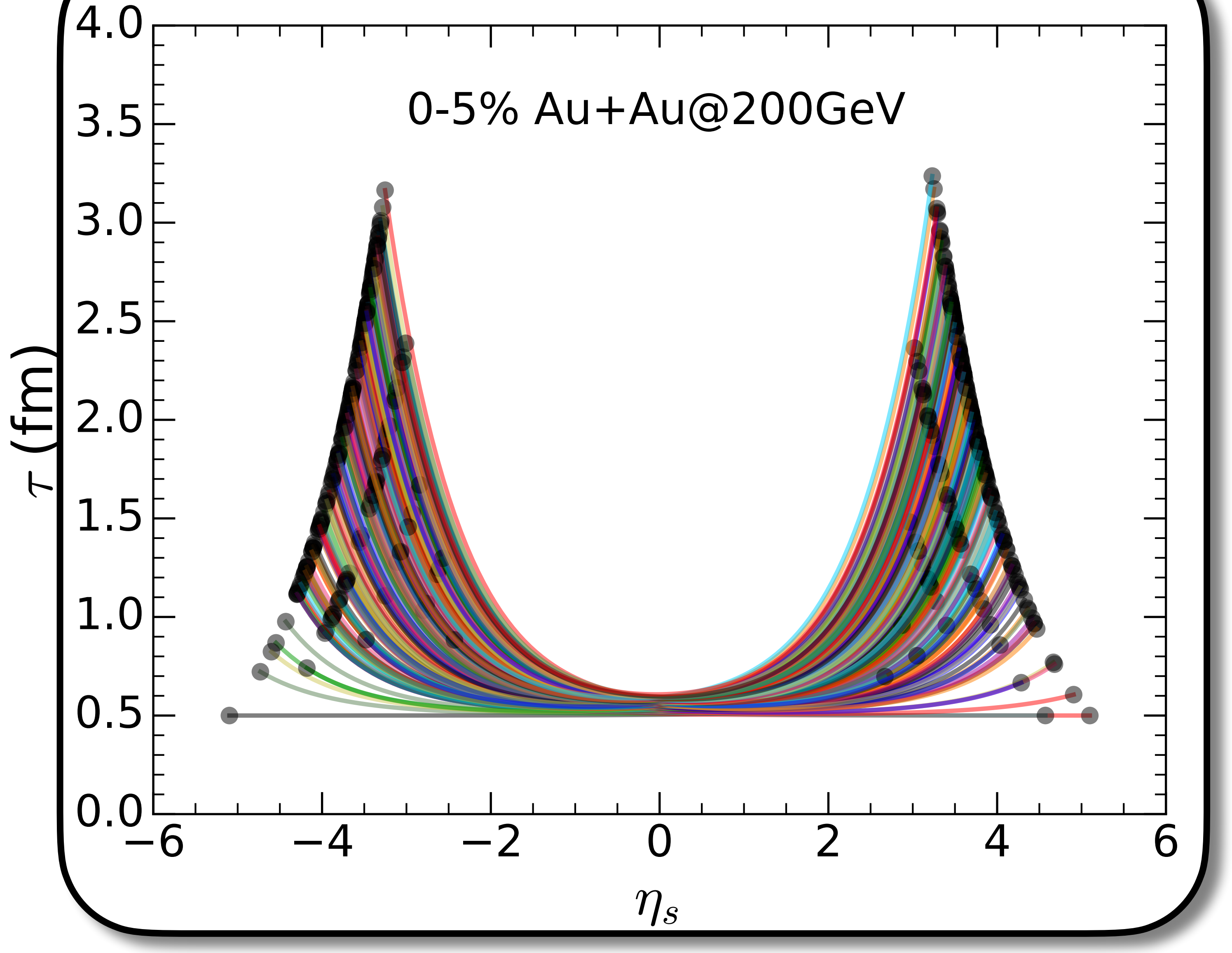


String deceleration

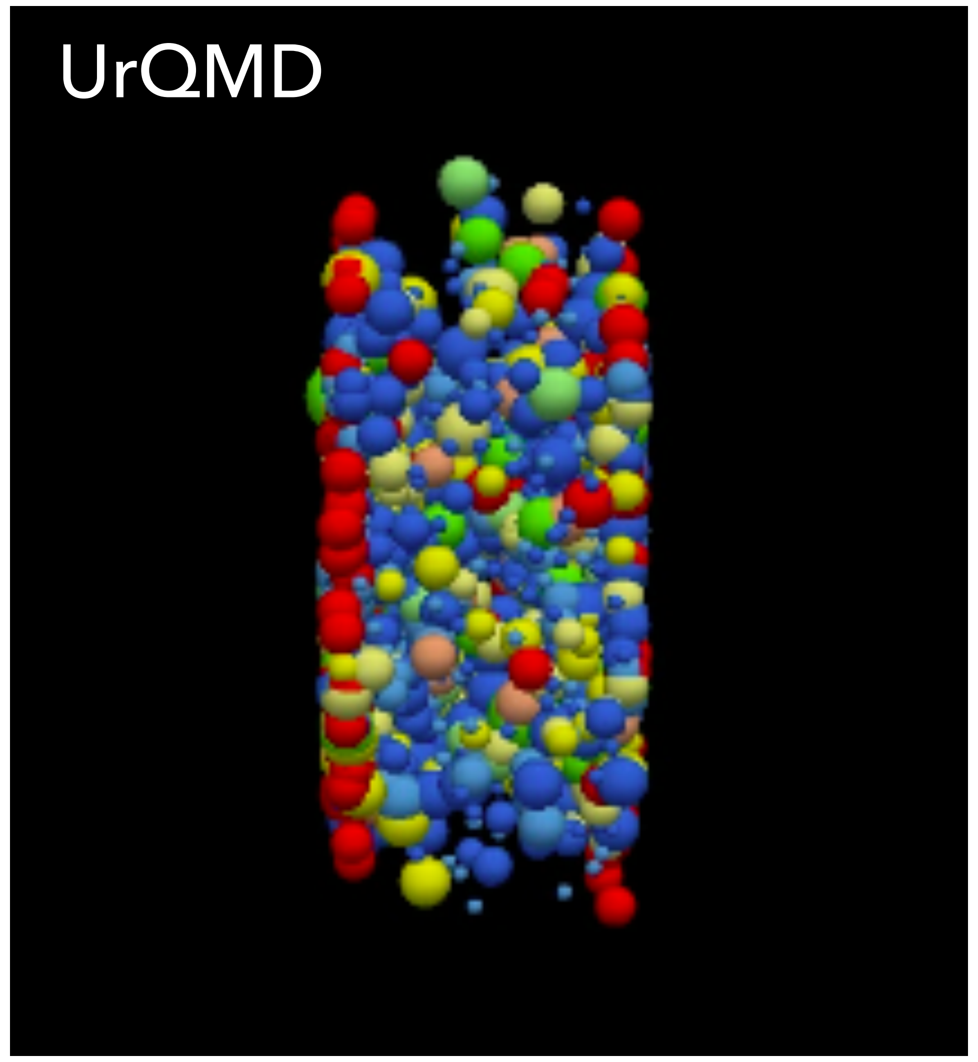


Transport + smearing kernel

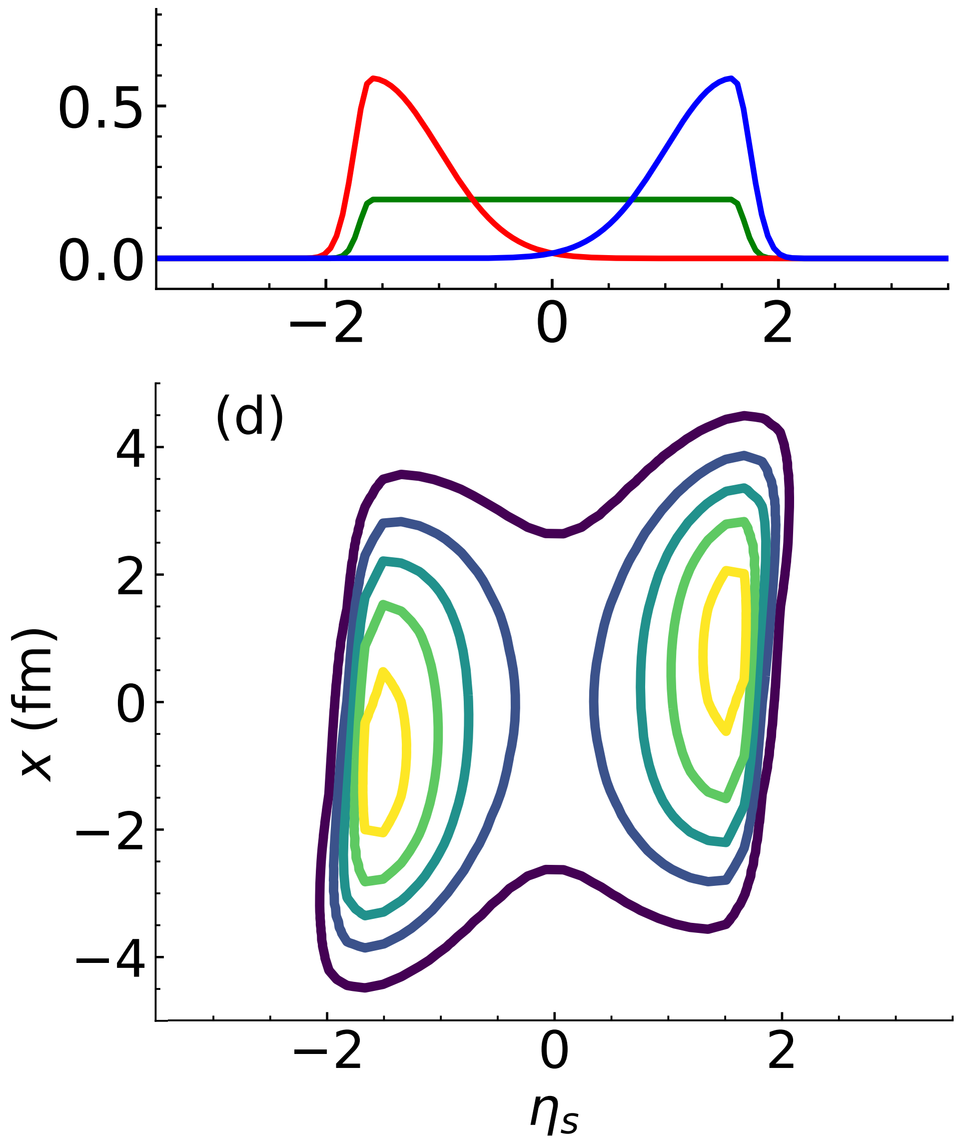


Parametric profiles + Glauber

- String deceleration (3D Glauber)
- Transport model + smearing kernel
- Geometry-based Glauber + parametric profiles
- …

C. Shen and S. Alzhrani, Phys. Rev. C 102, 014909 (2020); C. Shen and B. Schenke, Phys.Rev. C97 (2018) 024907; I. A. Karpenko, P. Huovinen, H. Petersen and M. Bleicher, Phys. Rev. C91 (2015) 064901; L. Du, U. Heinz and G. Vujanovic, Nucl. Phys. A982 (2019) 407-410; LD, C. Shen, S. Jeon & C. Gale, PRC 108 (2023) L041901; Garcia-Montero, Elfner, Schlichting, PRC 109 (2024) 4, 044916; Cimerman, Karpenko, Tomasik, Huovinen, PRC 107 (2023) 4, 4; … and many other advancements

# MID-RAPIDITY MEASUREMENTS

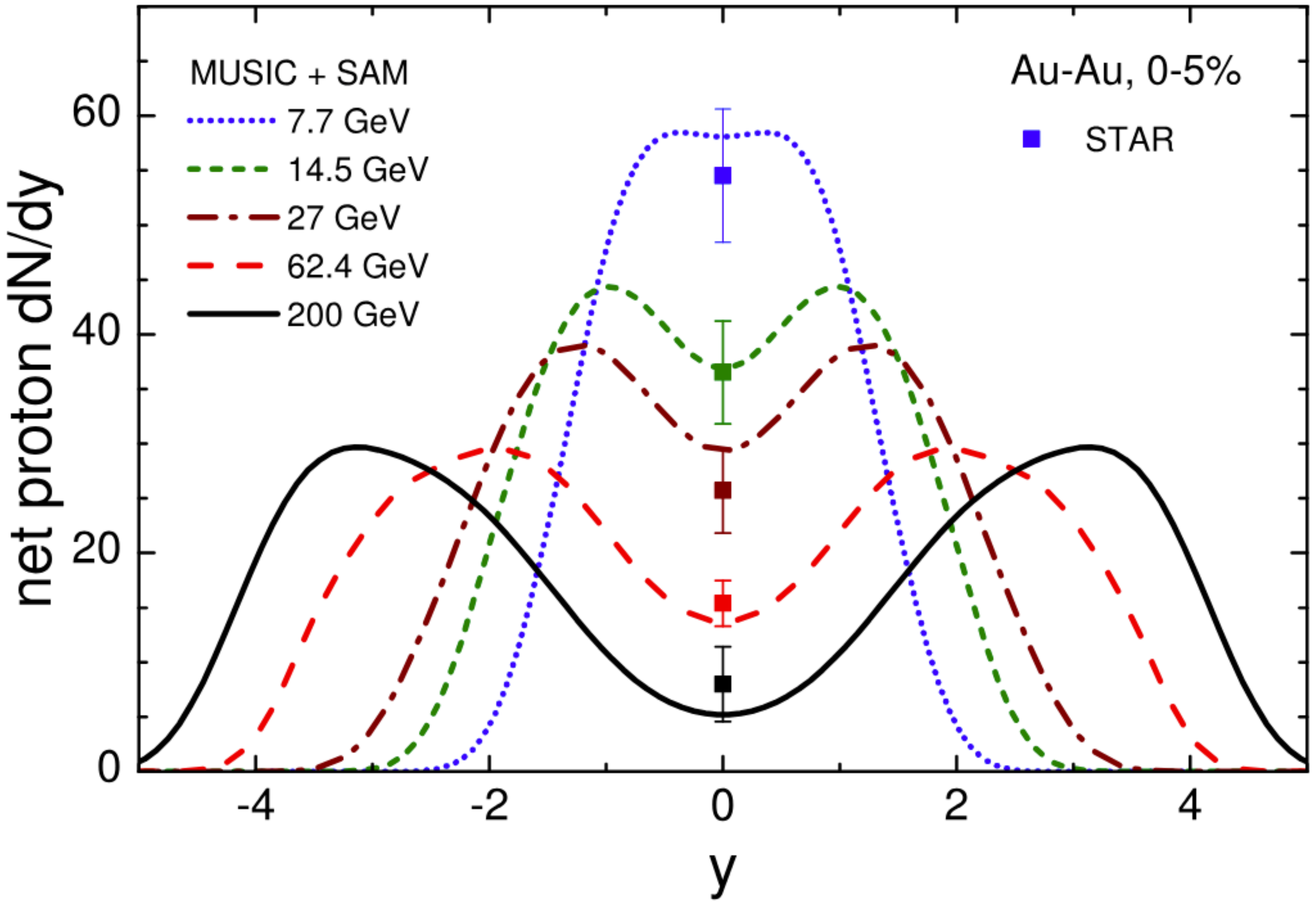


Vovchenko, Koch, and C. Shen, PRC 105, 014904 (2022)

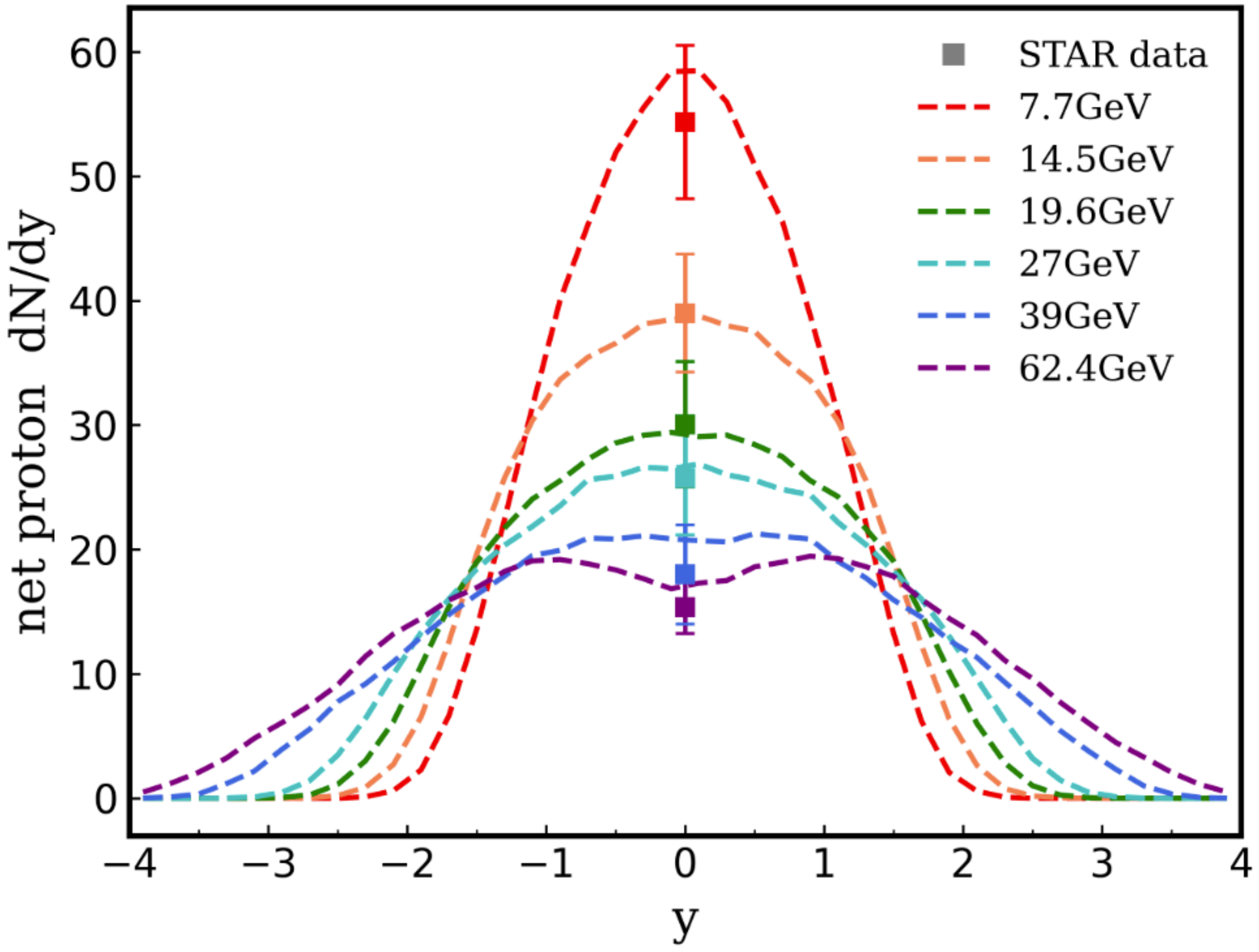


Y.-f. Shen, Chen, Wu, Xu, and Huang, PRC 111 (2025) 1, 014916

- If we only take measurements at mid-rapidity, the dynamics along the beam direction may not be well-constrained.

G. Denicol et al, PRC 98, 034916 (2018); LD, An and Heinz, PRC 104, 064904 (2021); LD, Gao, Jeon & Gale, PRC 109, 014907 (2024); Mendenhall and Lin, PRC 107, 034909 (2023); Cimerman, Karpenko, Tomášik, and Trzeciak, PRC 103, 034902 (2021); Cimerman, Karpenko, Tomášik, and Huovinen, PRC 107, 044902 (2023)

# CONSTRUCT RAPIDITY-DISTRIBUTION: $dN^{\mathrm{ch}}/d\eta$

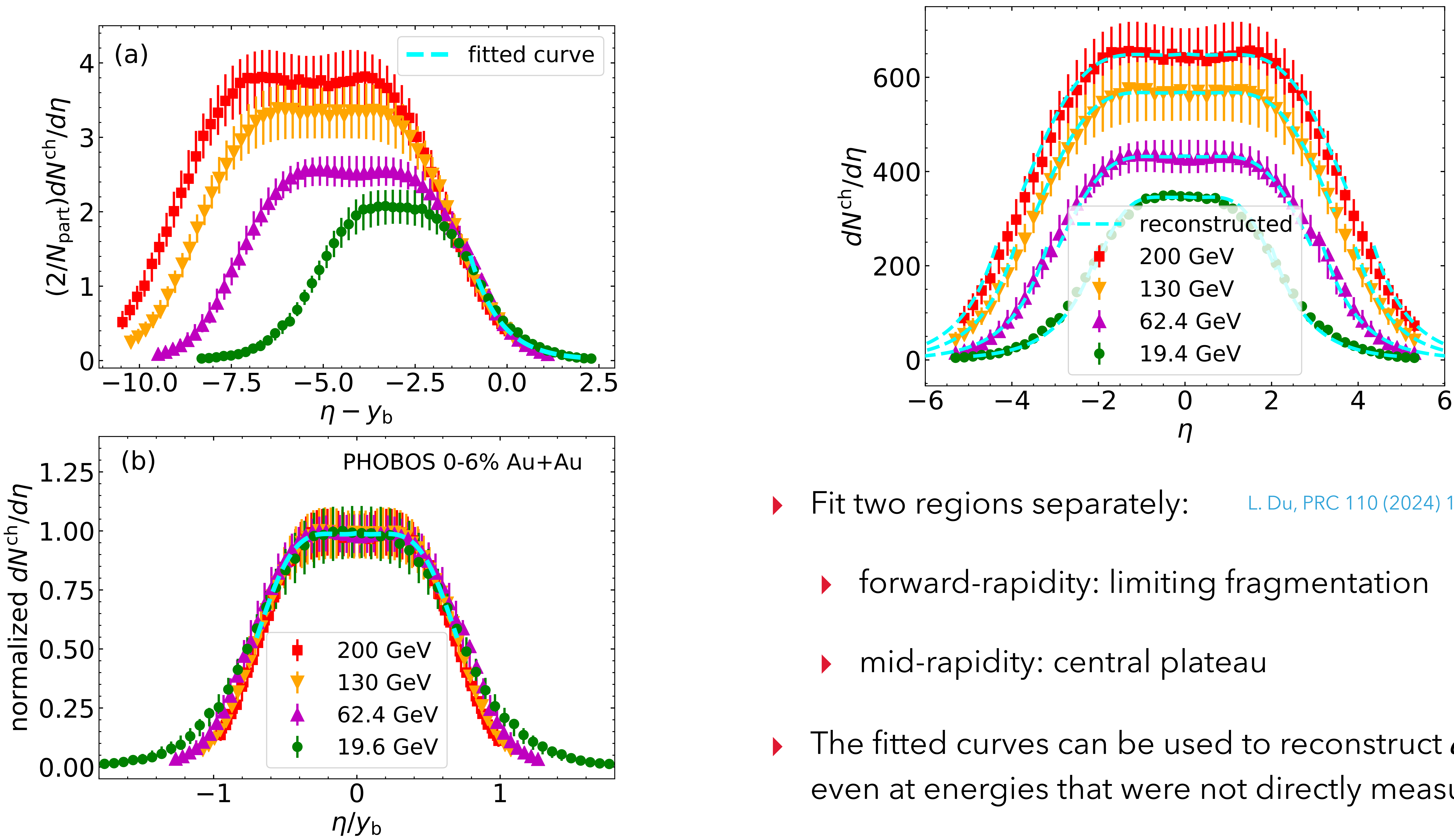


- Fit two regions separately: L. Du, PRC 110 (2024) 1, 014904
  - forward-rapidity: limiting fragmentation
  - mid-rapidity: central plateau
- The fitted curves can be used to reconstruct $dN^{\mathrm{ch}}/d\eta$, even at energies that were not directly measured.

PHOBOS, PRL 91, 052303 (2003); PHOBOS, PRC 83, 024913 (2011); ALICE, PRL 116, 222302 (2016); Basu et al 2021 J. Phys. G: Nucl. Part. Phys. 48 025103;

# CONSTRUCT RAPIDITY-DISTRIBUTION: $dN^{p-\bar{p}}/dy$

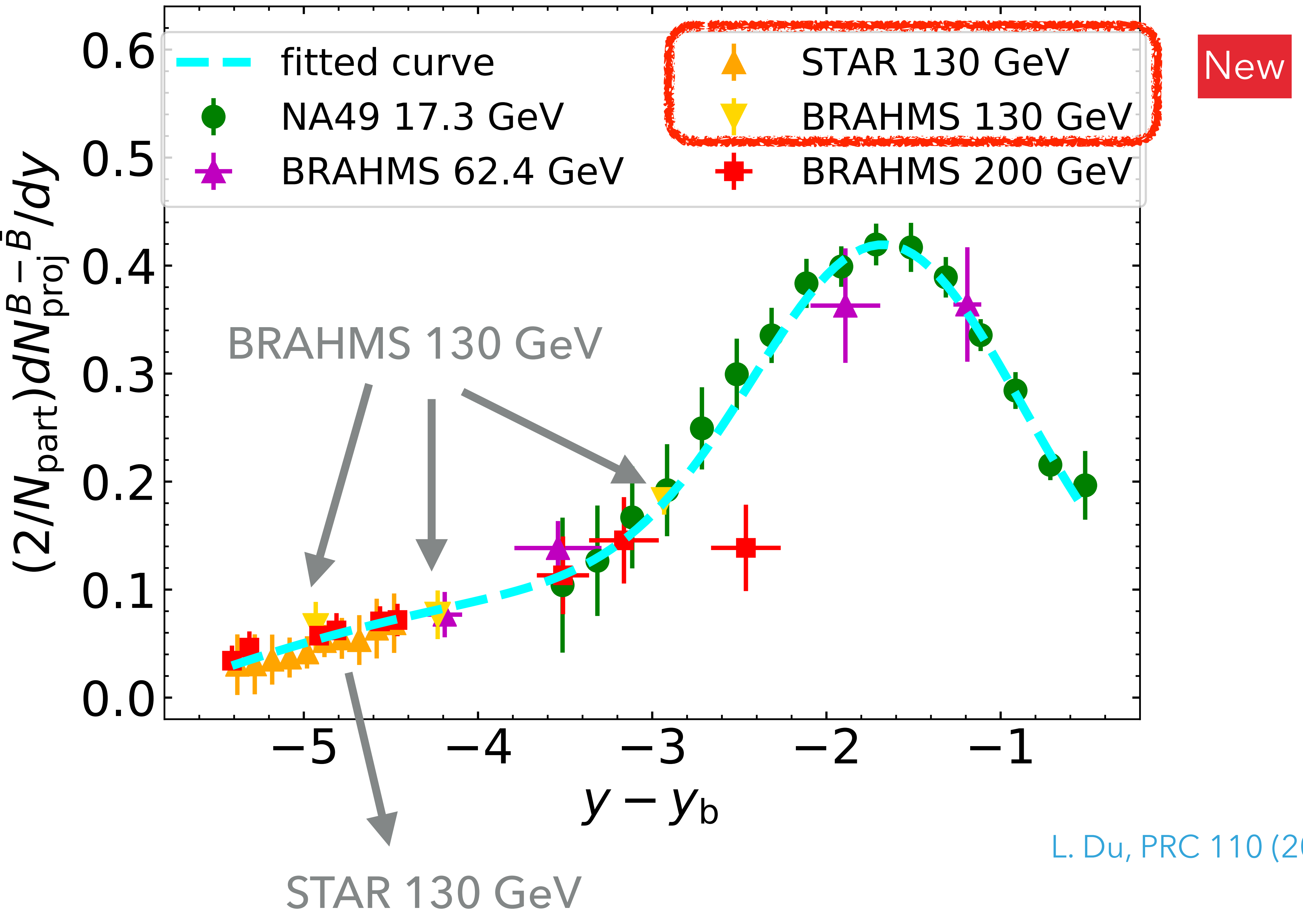


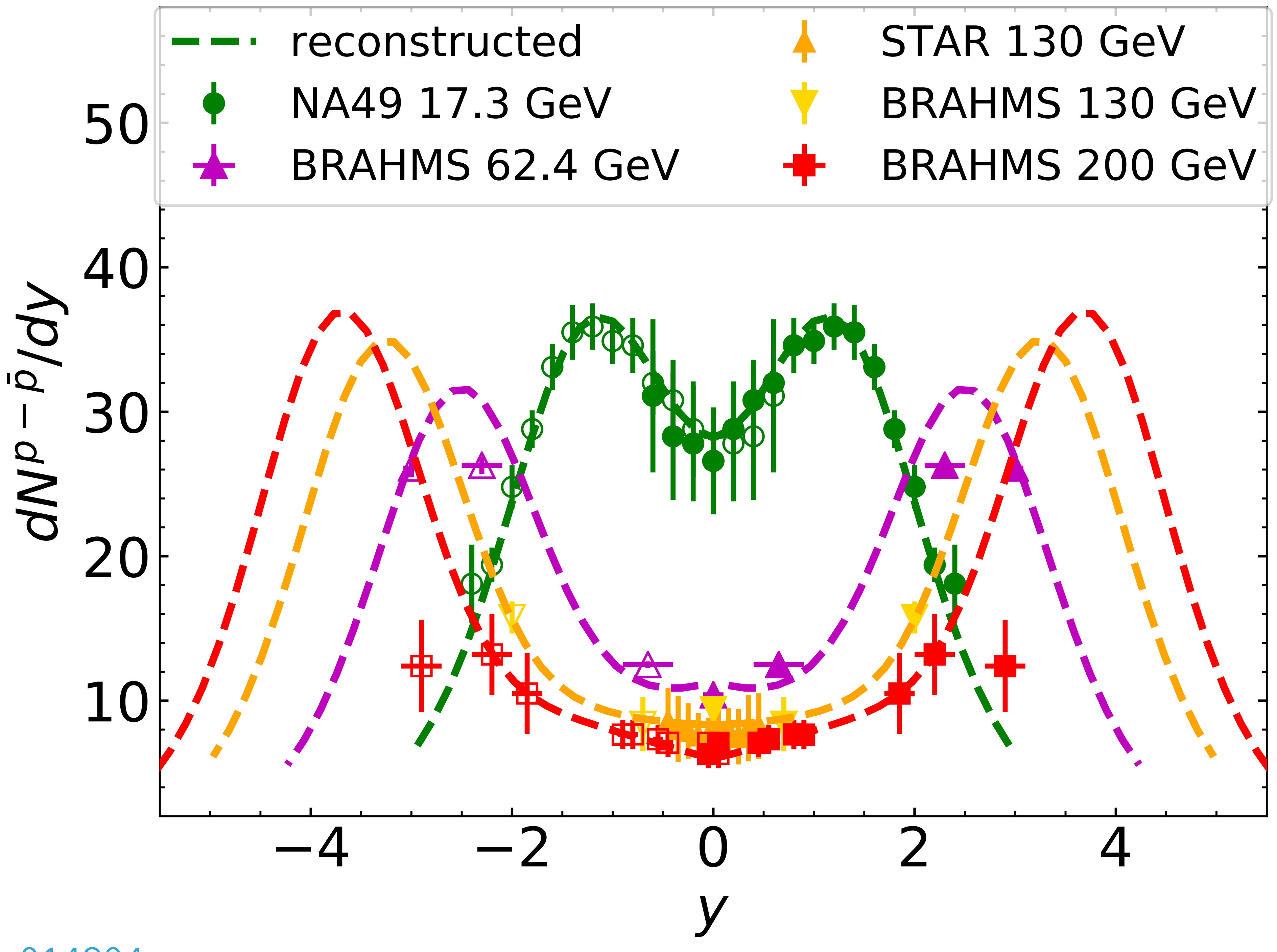


L. Du, PRC 110 (2024) 1, 014904

- Fit the net baryon rapidity density attributed to the projectile after subtraction of the target contribution.
- The reconstructed distributions can help constrain models at BES.

BRAHMS, PLB 677, 267-271(2009); Braun-Munzinger, Friman, Redlich, Rustamov, and Stachel, NPA 1008 (2021) 122141; Hoelck, Hiyama, and Wolschin, PLB 840, 137866 (2023)

# LONGITUDINAL FLOW AT FREEZE-OUT



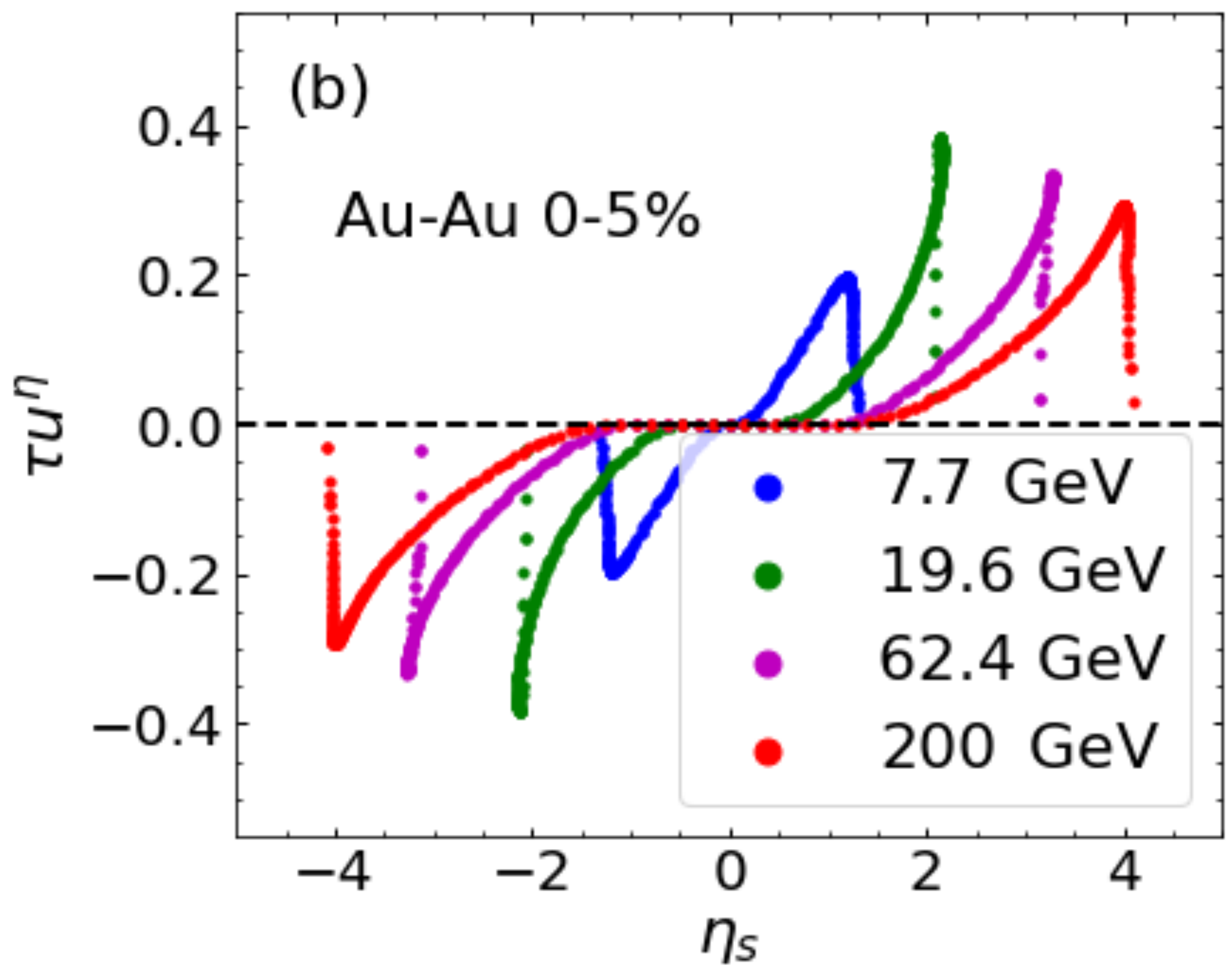


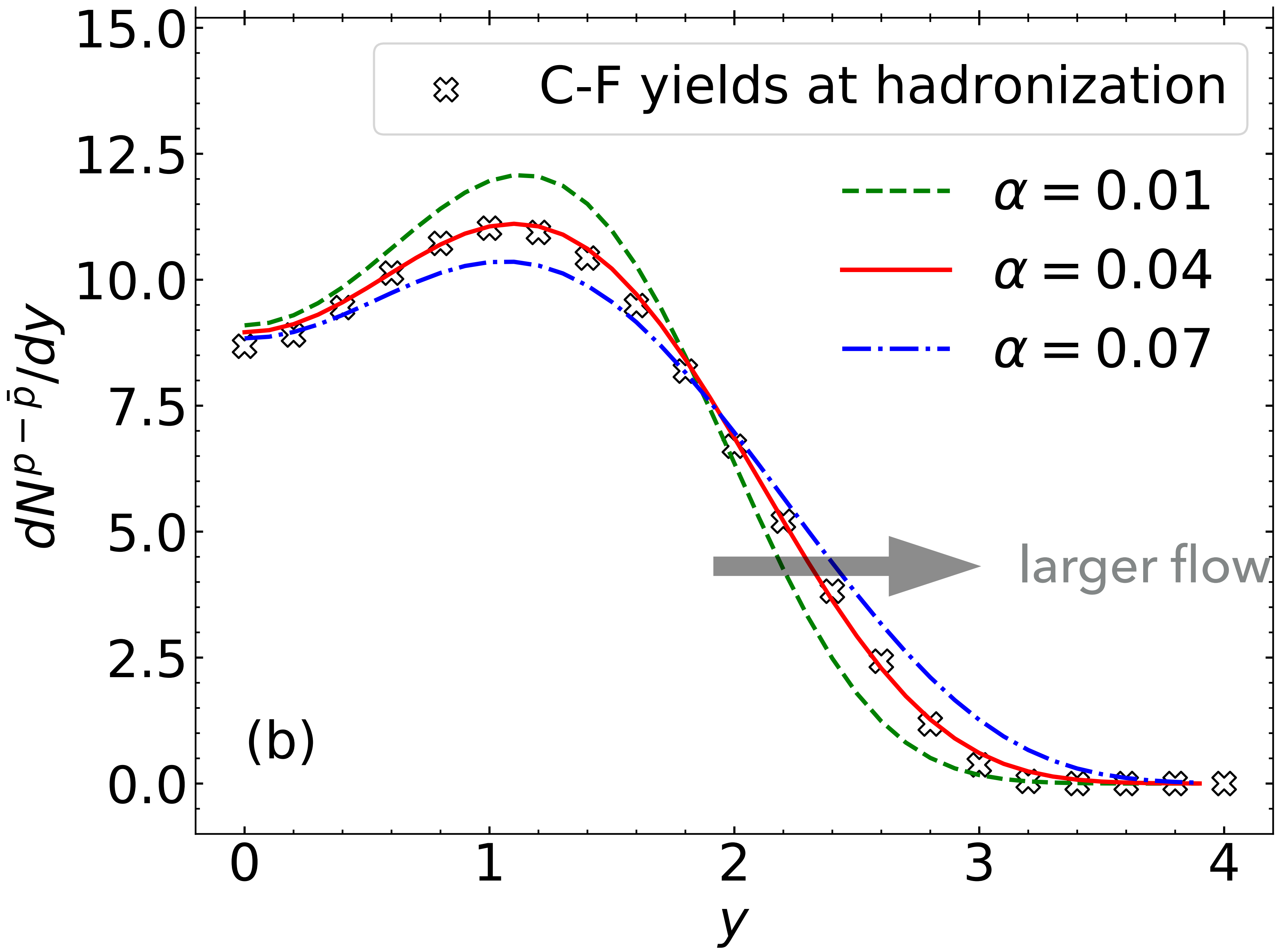


LD, H. Gao, S. Jeon & C. Gale, PRC 109, 014907 (2024)

- Boost invariance is strongly broken, especially at forward-/backward- rapidities;
- Starting from the same profiles, the rapidity distributions are stretched with increased longitudinal flow, with heavier particles experiencing greater stretching;
- Rapidity distributions of various species can be used to constrain the longitudinal flow.

# LONGITUDINAL PROPERTY VARIATION AT FREEZE-OUT

0-5% 7.7 GeV

$\Delta T/T_{\rm mid} \sim 20\,\%$

$\Delta\mu/\mu_{\rm mid} \gtrsim 100\,\%$

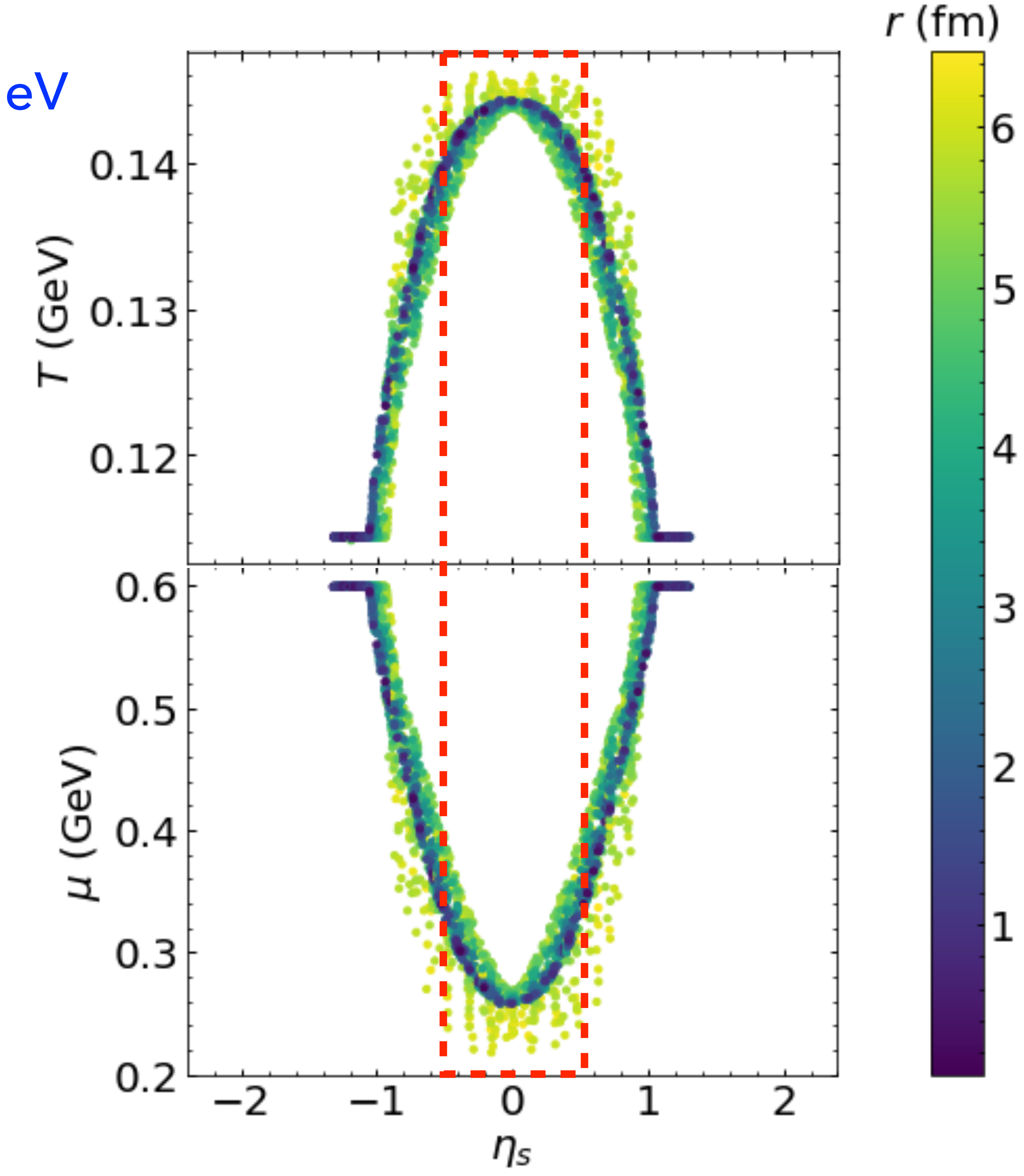


LD, H. Gao, S. Jeon & C. Gale, PRC 109, 014907 (2024)

0-10% BES

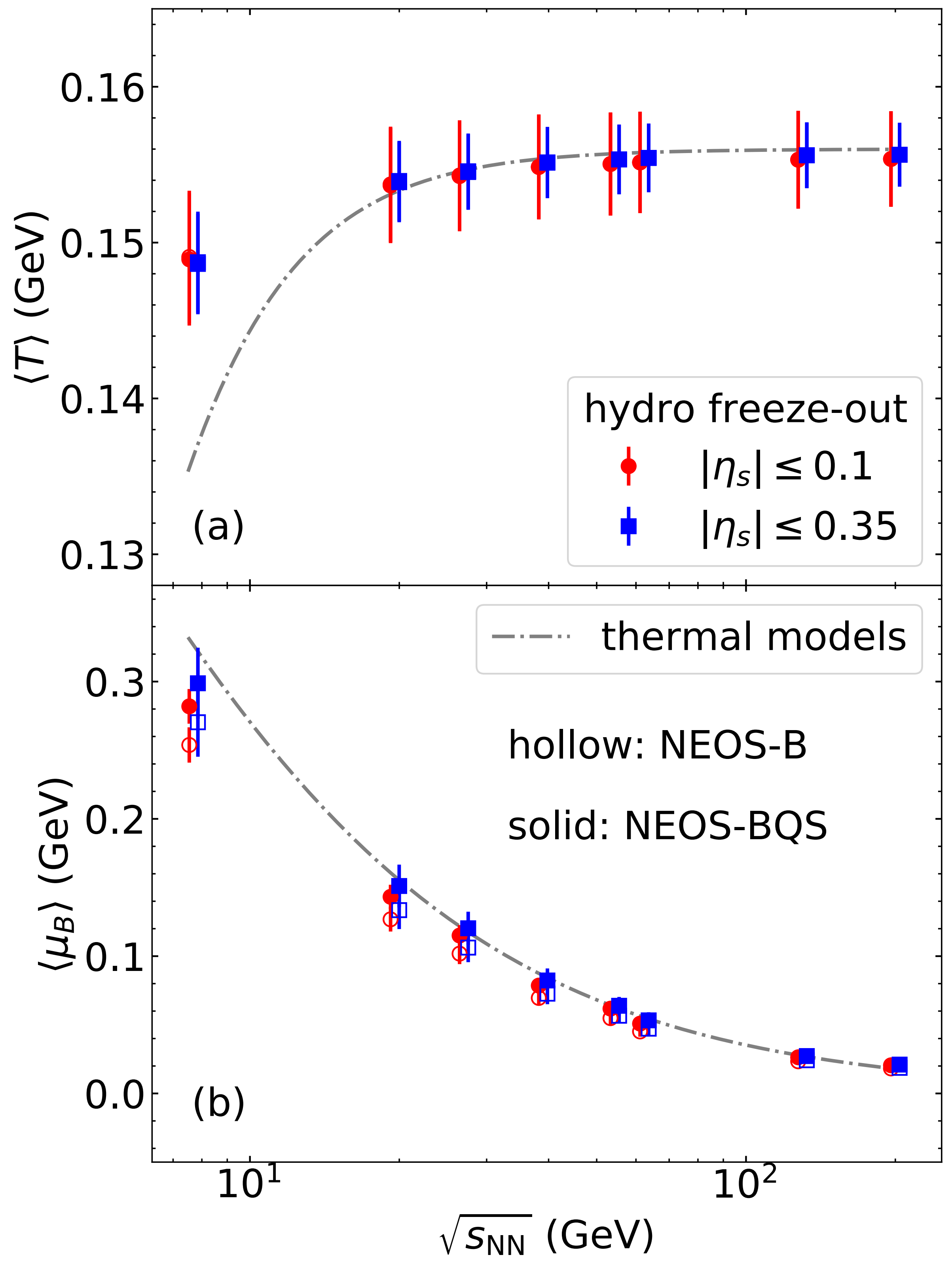


L. Du, PRC 110 (2024) 1, 014904

- The variation in thermodynamic properties across spacetime rapidity is strong for collisions $\lesssim$10 GeV
- Due to thermal smearing, thermal models extract $(T, \mu_B)$ averaged over a broader $\eta_s$ window

Andronic, Braun-Munzinger, Redlich, and Stachel, Nature 561, 321–330 (2018); Begun, Kikoła, Vovchenko, and Wielanek, PRC 98, 034905 (2018); Karpenko, Acta Phys. Polon. B50 (2019), 141

# FREEZE-OUT

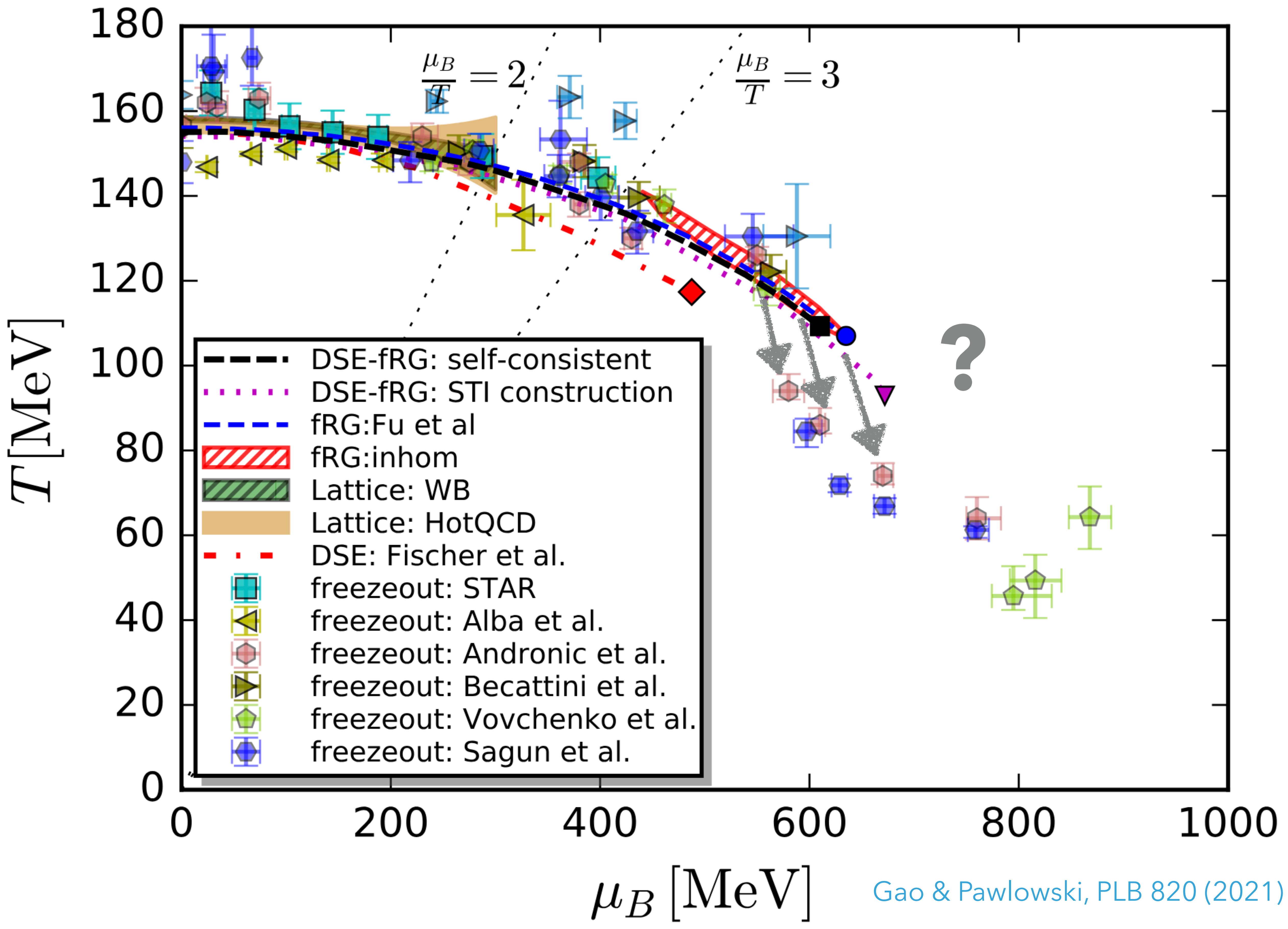


Gao & Pawlowski, PLB 820 (2021) 136584

- An indication of $(T, \mu_B)$ averaged over a broader $\eta_s$ window?
- Essential to consider the rapidity-variation of thermodynamic properties

# BEAM ENERGY SCAN VS. RAPIDITY SCAN



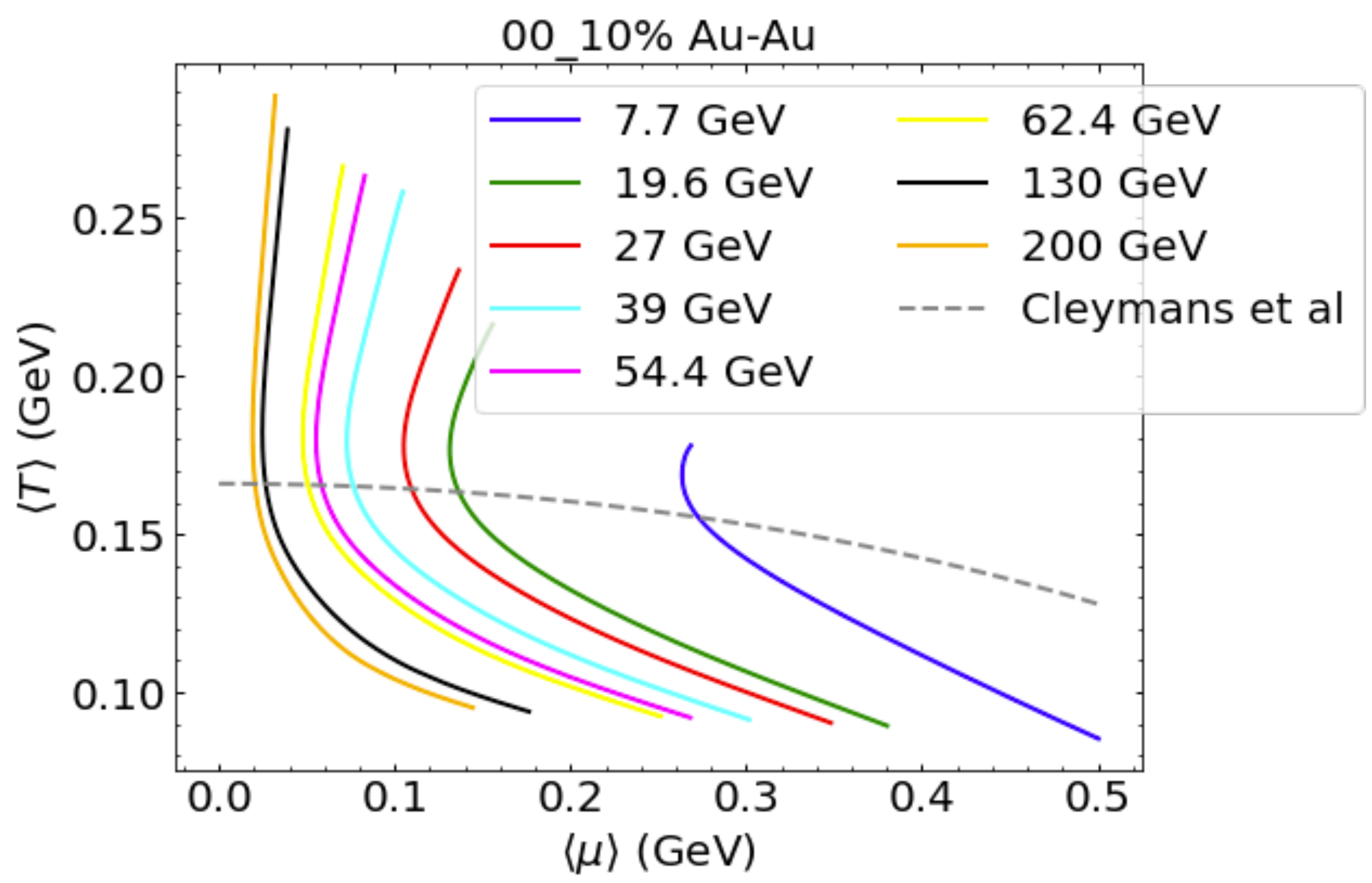


properties averaged over a rapidity window

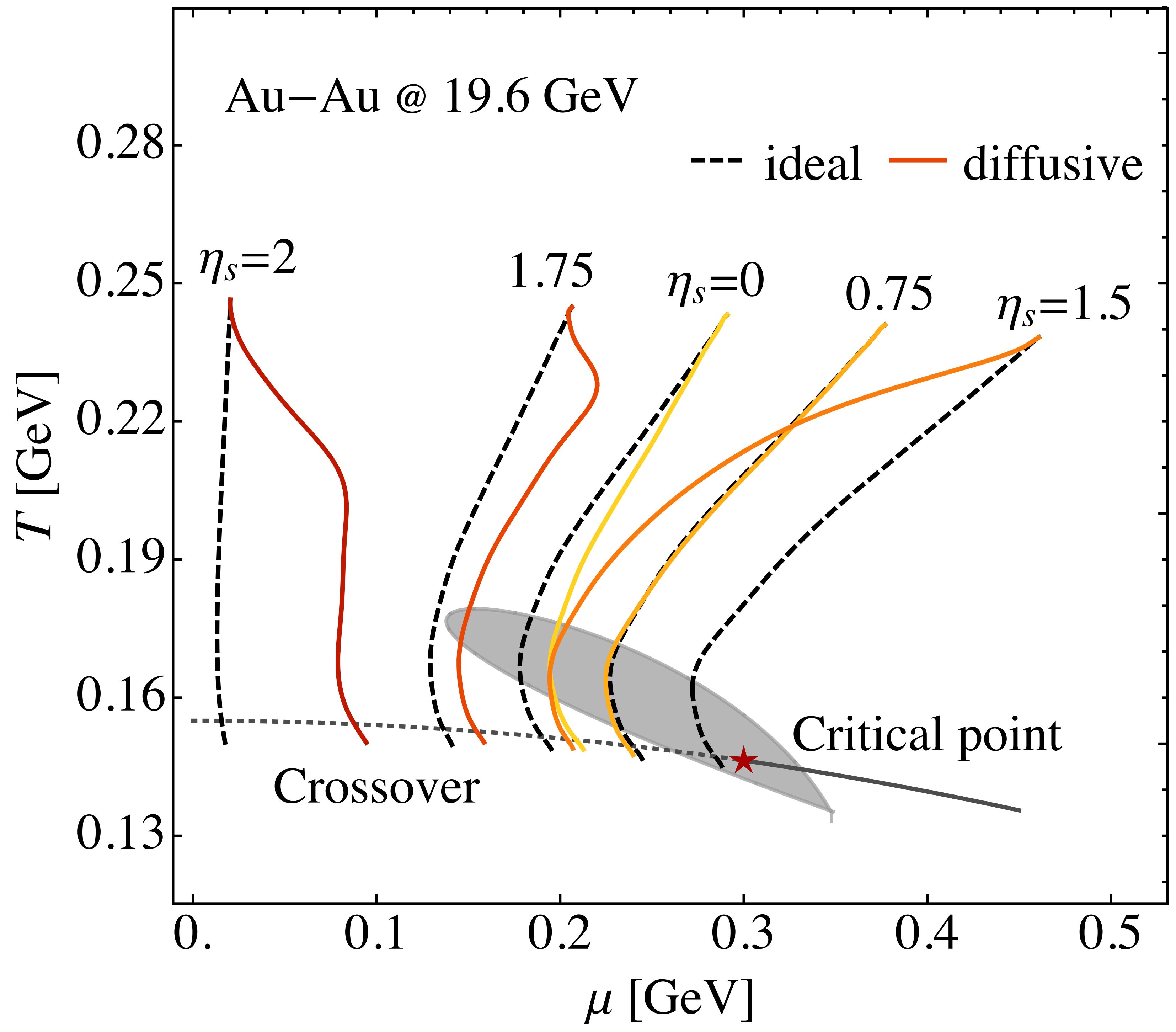


LD, X. An and U. Heinz, PRC 104, 064904 (2021); CPOD21, 2109.06918

- Left: expansion trajectories at midrapidity in heavy-ion collisions with different beam energies;
- Right: expansion trajectories for different rapidities of the fireball in a collision at a fixed beam energy

# RAPIDITY SCAN: (3+1)D

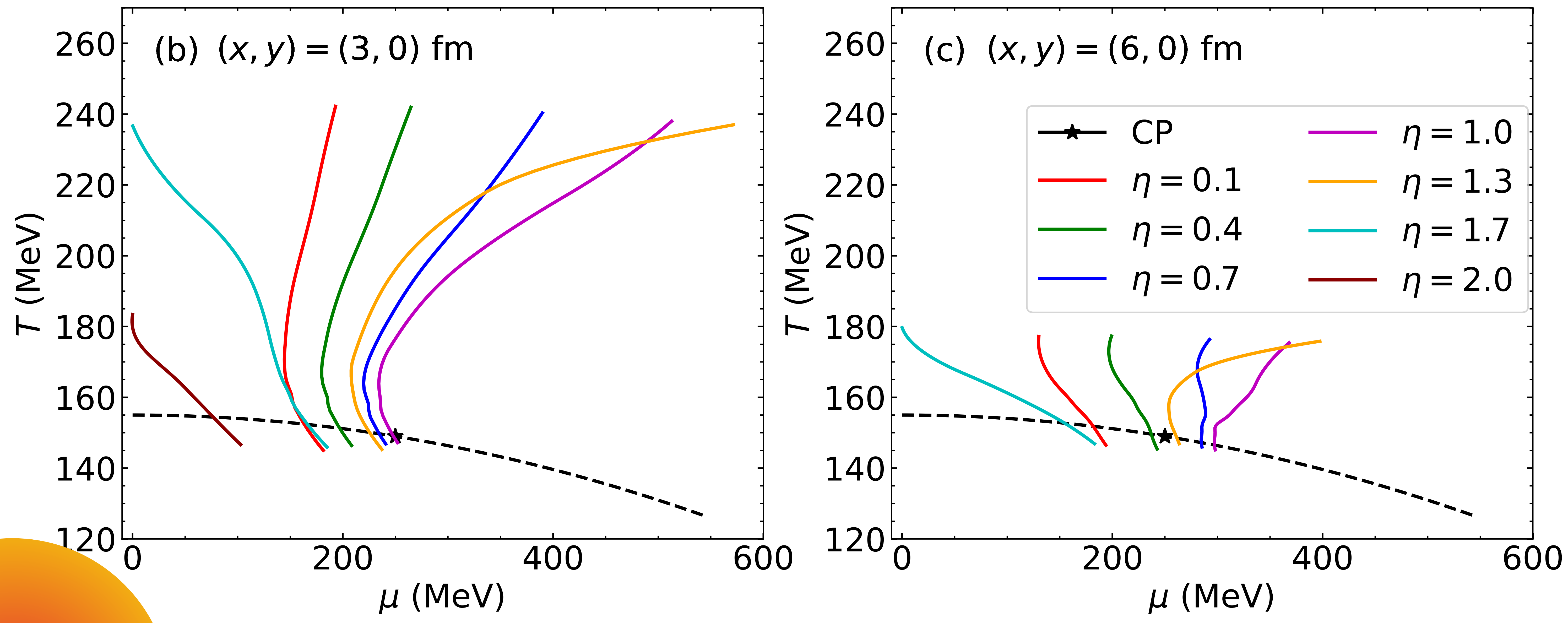


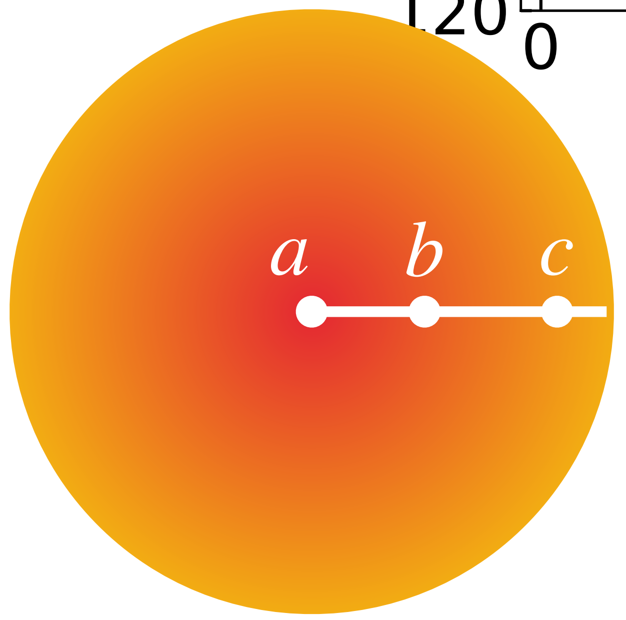


Phase diagram trajectories in a (3+1)D evolution

LD, X. An and U. Heinz, PRC 104, 064904 (2021); CPOD21, 2109.06918

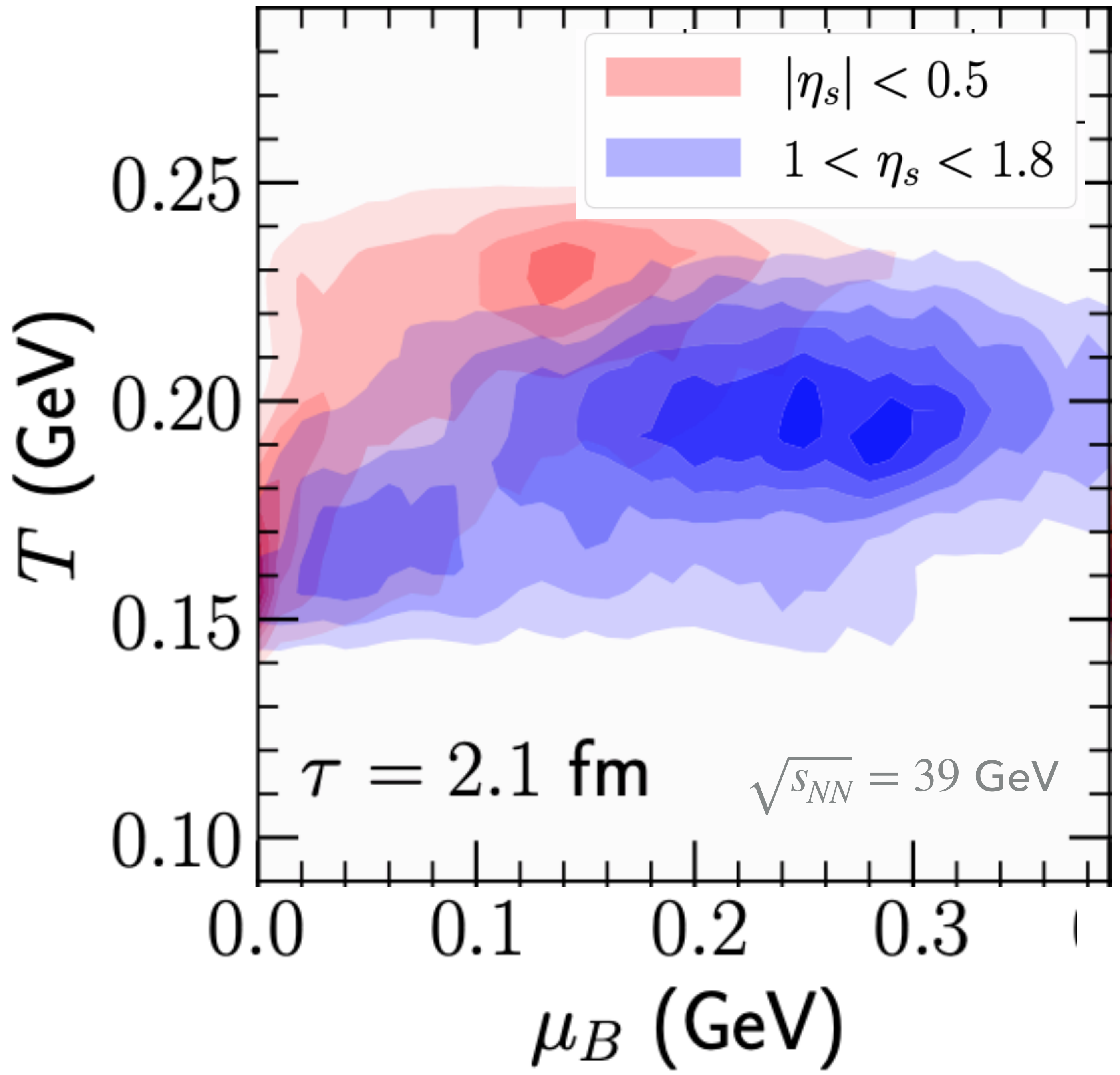


C. Shen: 2108.04987

- The phase diagram trajectories are complex due to the dynamic and inhomogeneous nature of the QCD matter produced in heavy-ion collisions.
- What fraction of the system volume probes the critical region at a given beam energy?

# MULTI-CHARGE FLUID

- Three types of conserved charges in QCD: Baryon number (B), Electric charge (Q), and Strangeness (S);
- Hydrodynamic evolution of the multi-charge fluid

$$\partial_\mu N_q^\mu = 0\,, \quad N_q^\mu = n_q u^\mu + n_q^\mu\,, \quad q \in \{B, Q, S\}$$

$$\sum_{q'} \tau_{qq'} \dot{n}_{q'}^{\langle\mu\rangle} + n_q^\mu = \sum_{q'} \kappa_{qq'} \nabla^\mu \left(\frac{\mu_{q'}}{T}\right) + \text{(higher-order gradients)}$$

J. Jahan, Tue. 11:30 am

- Equation of State: $p = p(T, \mu_B, \mu_Q, \mu_S)$
- Necessary features of hydro codes: 3D, conservation & coupled diffusion of BQS charges, BQS-dependent transport coefficients and EoS, possible critical effects

MUSIC, BEShydro, CLvisc, vHLLE, CCAKE, three-fluid, …

# MULTI-CHARGE FLUID

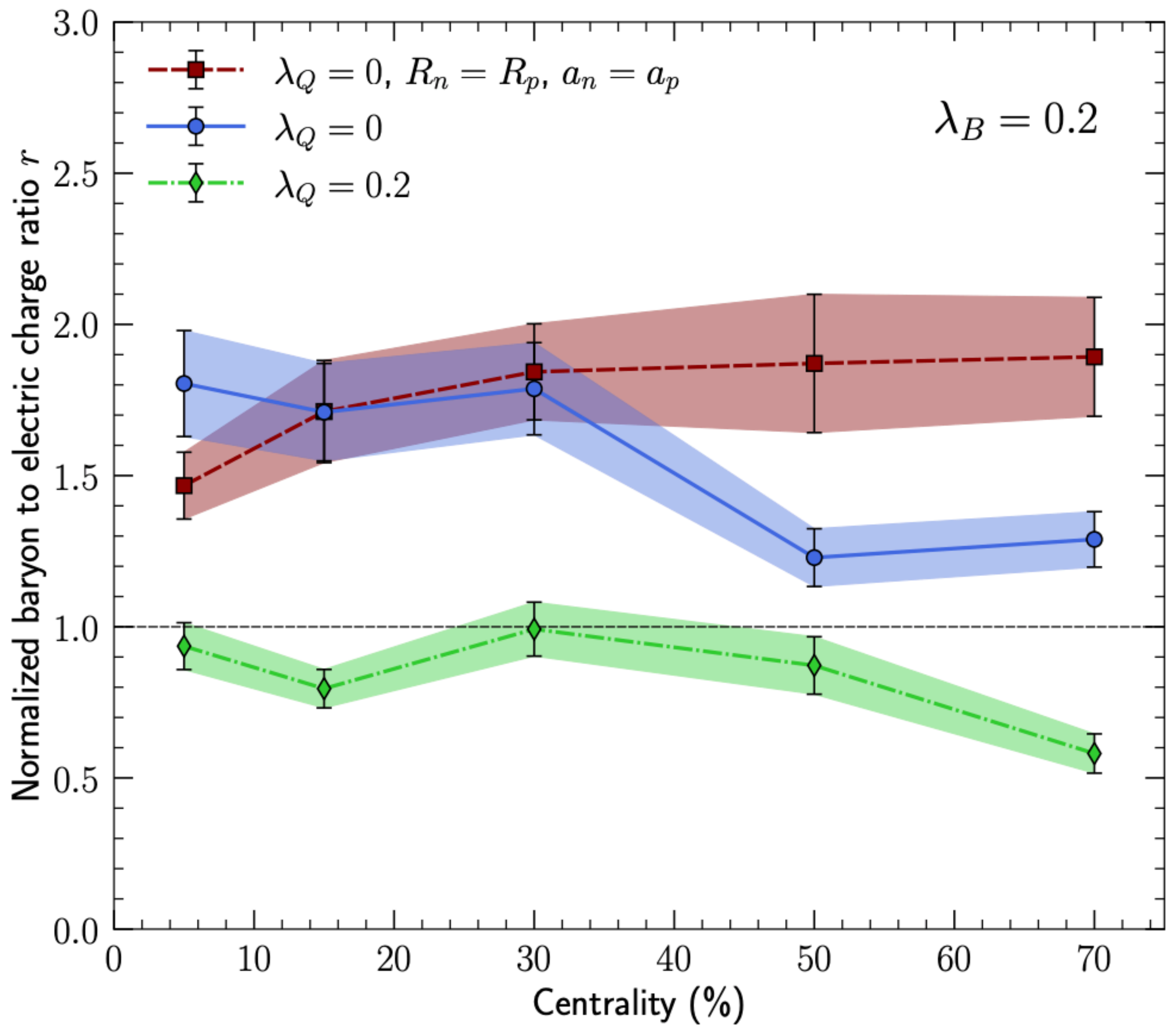


Pihan, Monnai, Schenke, and Shen, Phys.Rev.Lett. 133 (2024) 18, 182301

ICCING + CCAKE

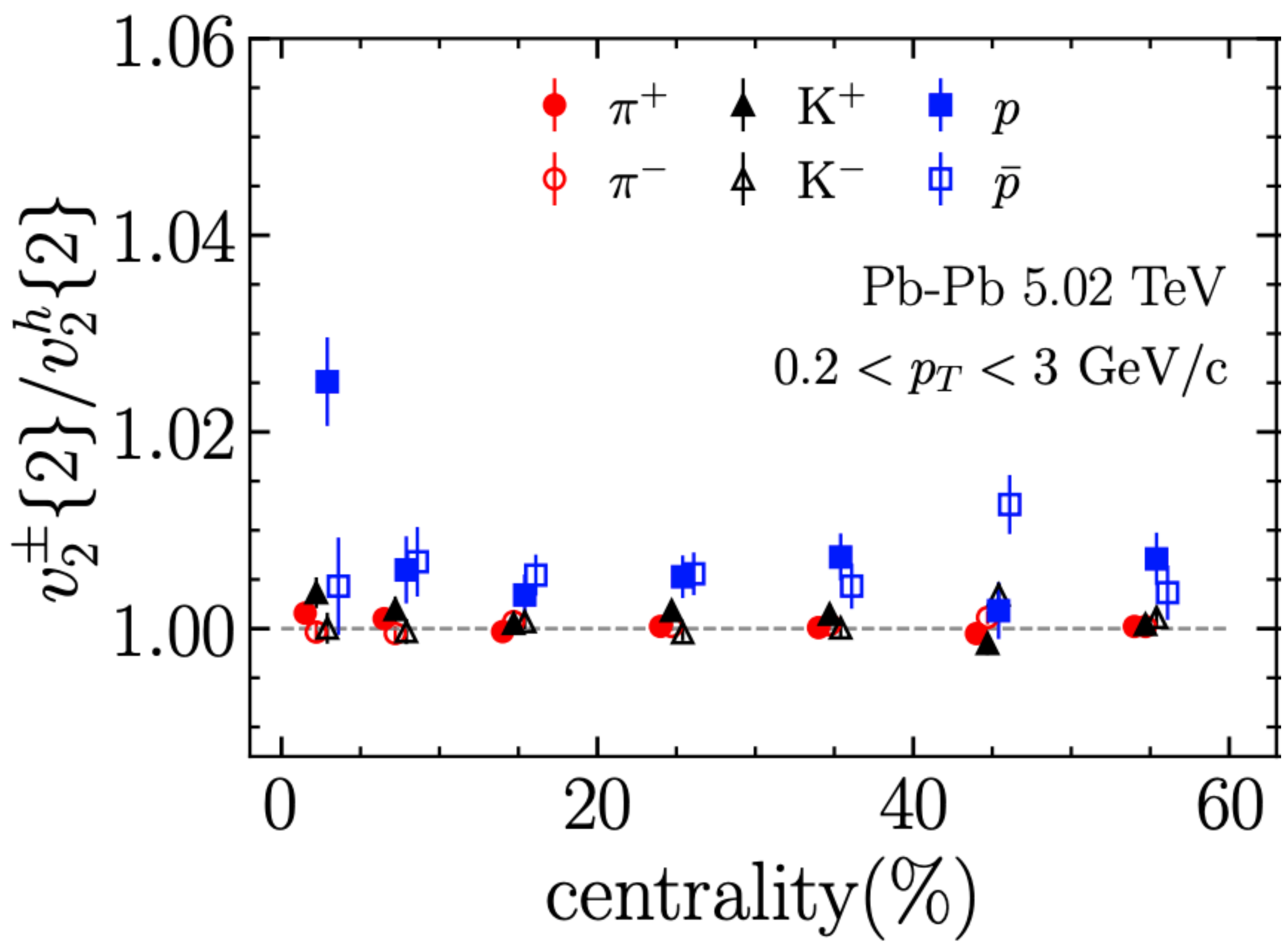


Gardim, Almaalol, Salinas San Martn, Plumberg, Noronha-Hostler, 2411.00590

- The baryon-to-electric charge ratio as a function of centrality could potentially reveal initial-state electric charge transport stopping.
- ICCING + CCAKE: gluons splitting into quark-antiquark pairs; new observables that quantify the effect of BSQ charge fluctuations that arise from such splittings in the initial state at the LHC

# PROBING EOS AT FINITE CHEMICAL POTENTIALS

NEOS: Monnai et al, PRC 100, 024907 (2019)

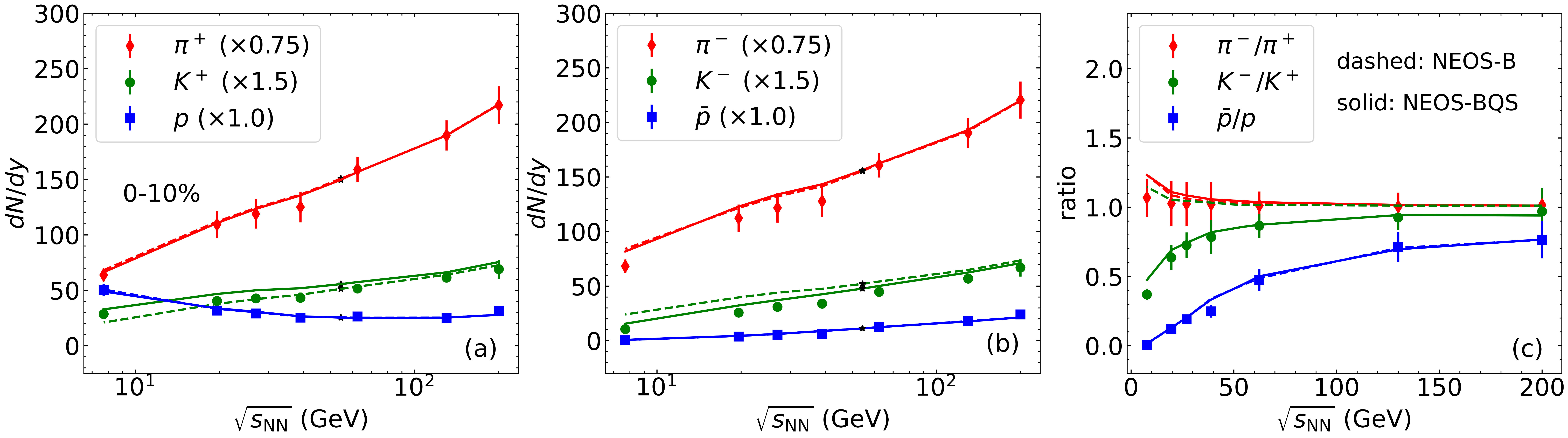


L. Du, PRC 110 (2024) 1, 014904

- Two limits of EoS: NEOS-B, $\mu_S = \mu_Q = 0$ and NEOS-BQS, $n_S = 0,\ n_Q = 0.4\,n_B$ (2D projection of a 4D EOS $p = p(T, \mu_B, \mu_Q, \mu_S)$)
- Ratios of $K^-/K^+ \propto \exp\left[-2(\mu_Q + \mu_S)\right]$  $K^+:\ \mu_Q + \mu_S,\quad K^-: -\mu_Q - \mu_S$

# PROBING EOS AT FINITE CHEMICAL POTENTIALS



NEOS: Monnai et al, PRC 100, 024907 (2019)

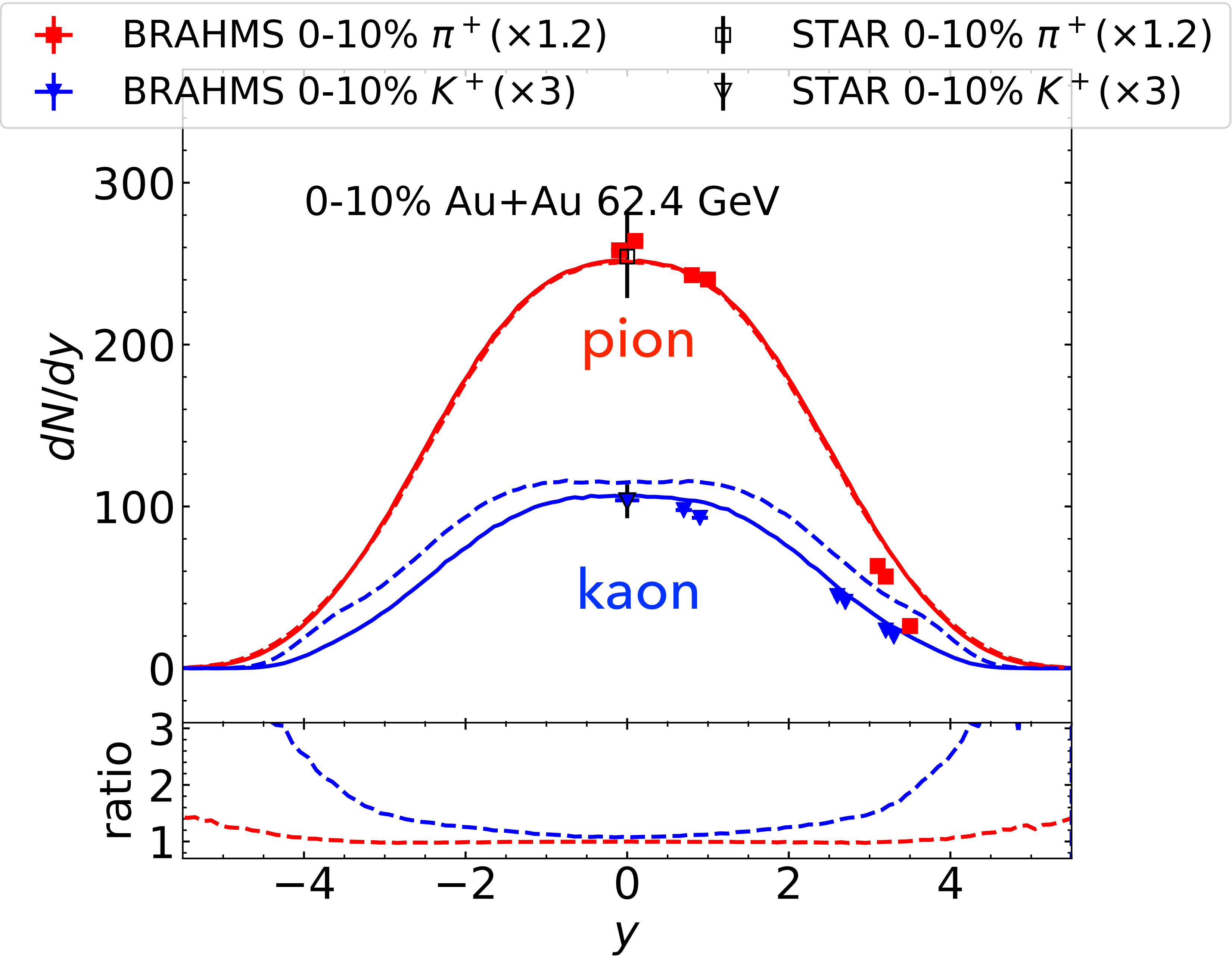


L. Du, PRC 110 (2024) 1, 014904

Dashed: NEOS-BQS

Solid: NEOS-B

Data: STAR, PRL 112, 162301 (2014); PRL 120, 062301 (2018)

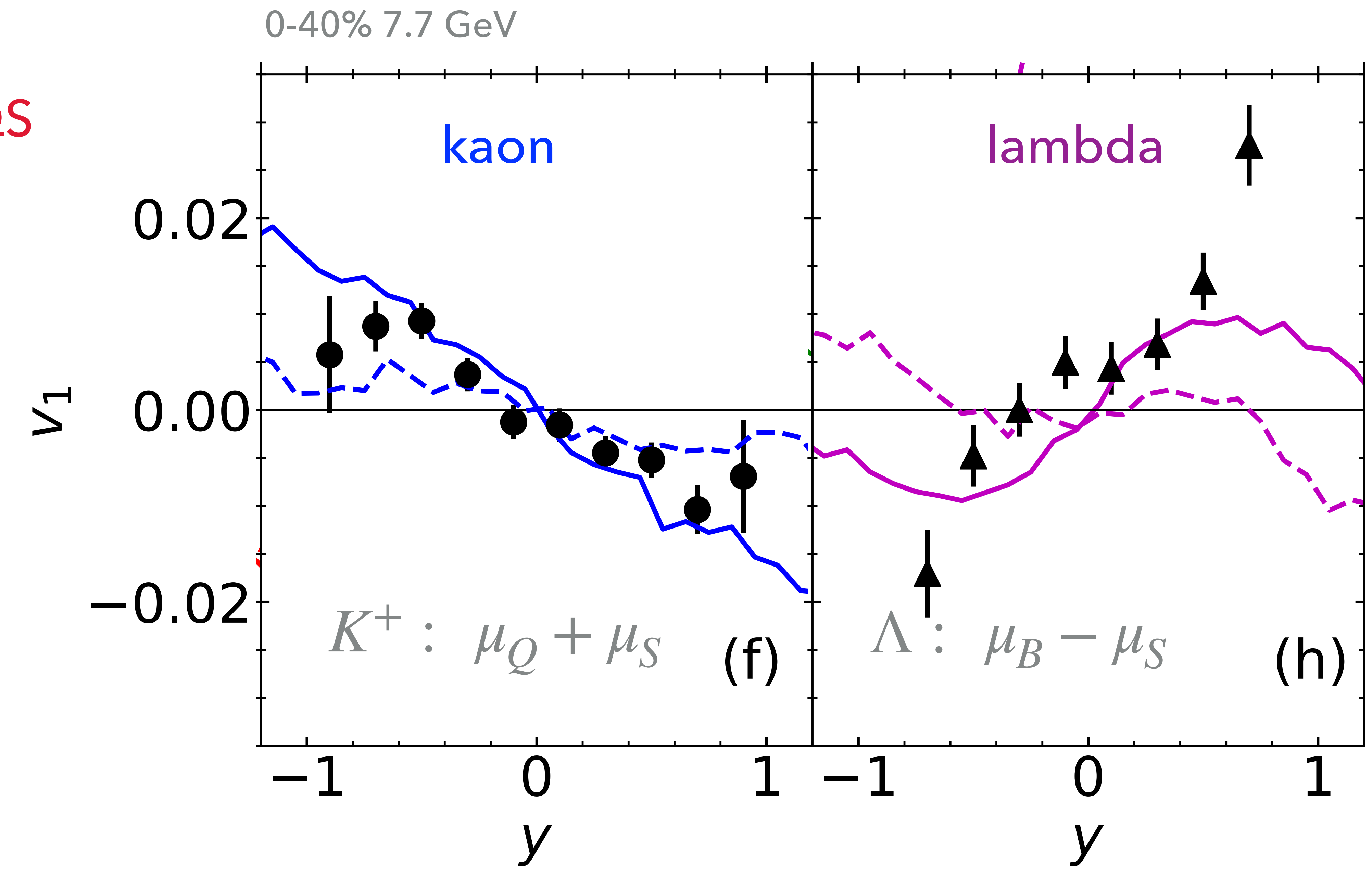


LD, C. Shen, S. Jeon & C. Gale, PRC 108 (2023) L041901

- Rapidity-dependent measurements of identified particles provide valuable insights into the EoS at finite chemical potentials.
- The directed flow of identified particles offers significant constraining power on the properties of the EoS.

# ELECTROMAGNETIC PROBES

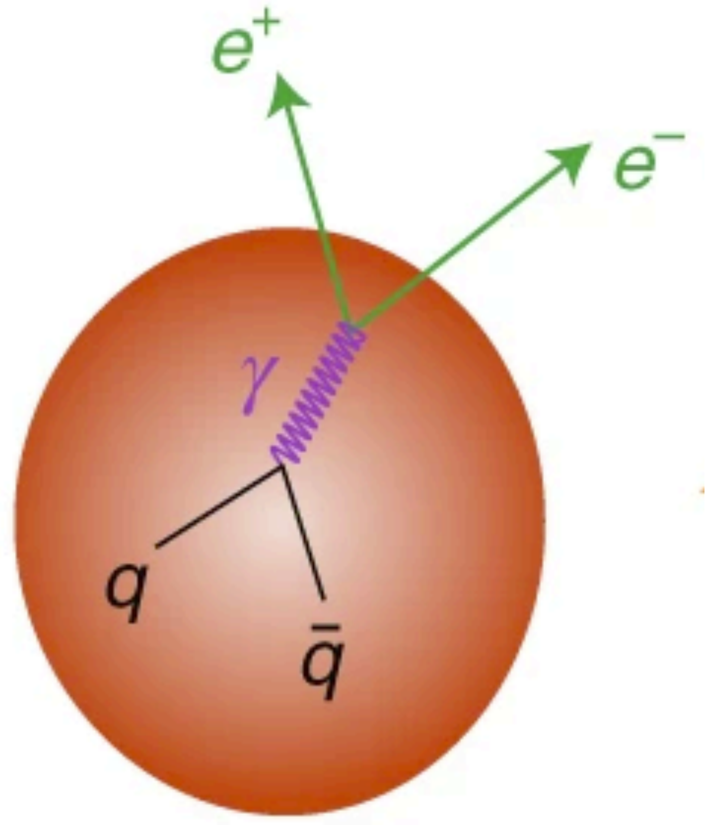


- Dileptons & real photons: A penetrating, “clean” probe
  - emitted throughout the entire evolution of the medium
  - escape the strongly interacting medium with negligible interactions (“clean”)

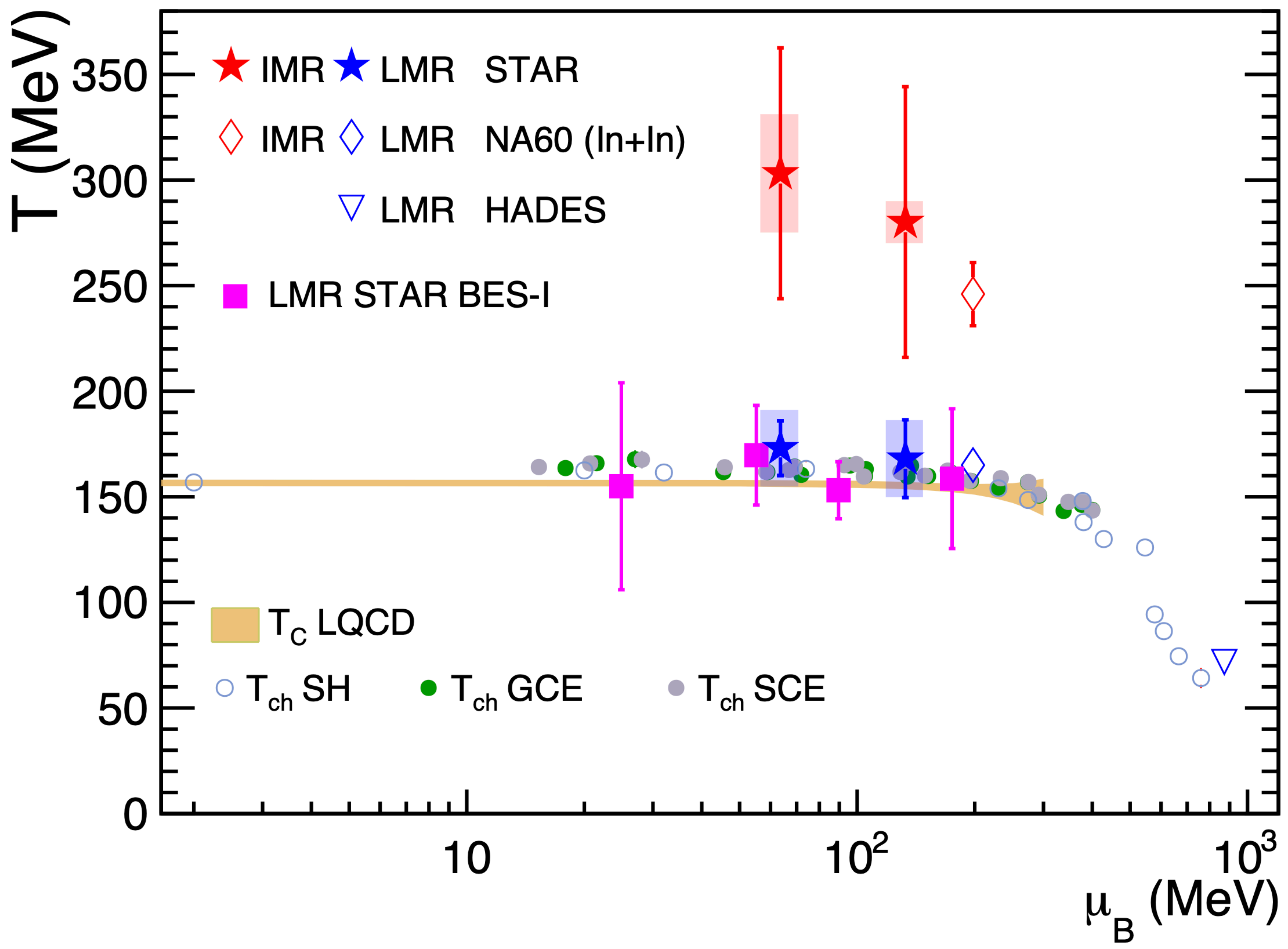


STAR, 2402.01998

NA60, PRL 100, 022302 (2008); EPJC 59 607-623 (2009). STAR, PRL113, 022301 (2014); PRC 92, 024912 (2015); PLB 750 (2015) 64–71; PRC 107, L061901 (2023). HADES, Nat. Phys.,1040–1045 (2019).

# THERMAL DILEPTON AS THERMOMETER

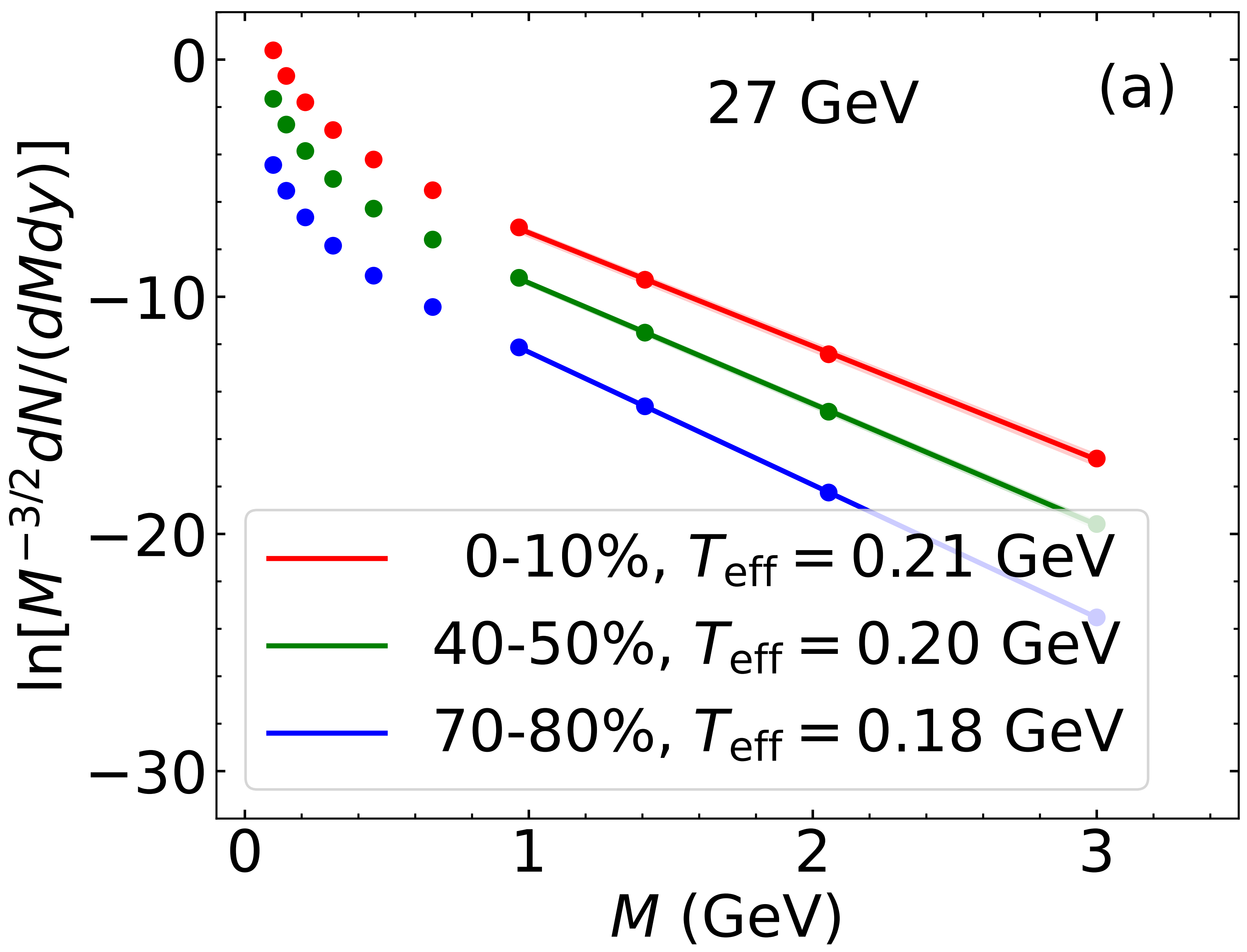


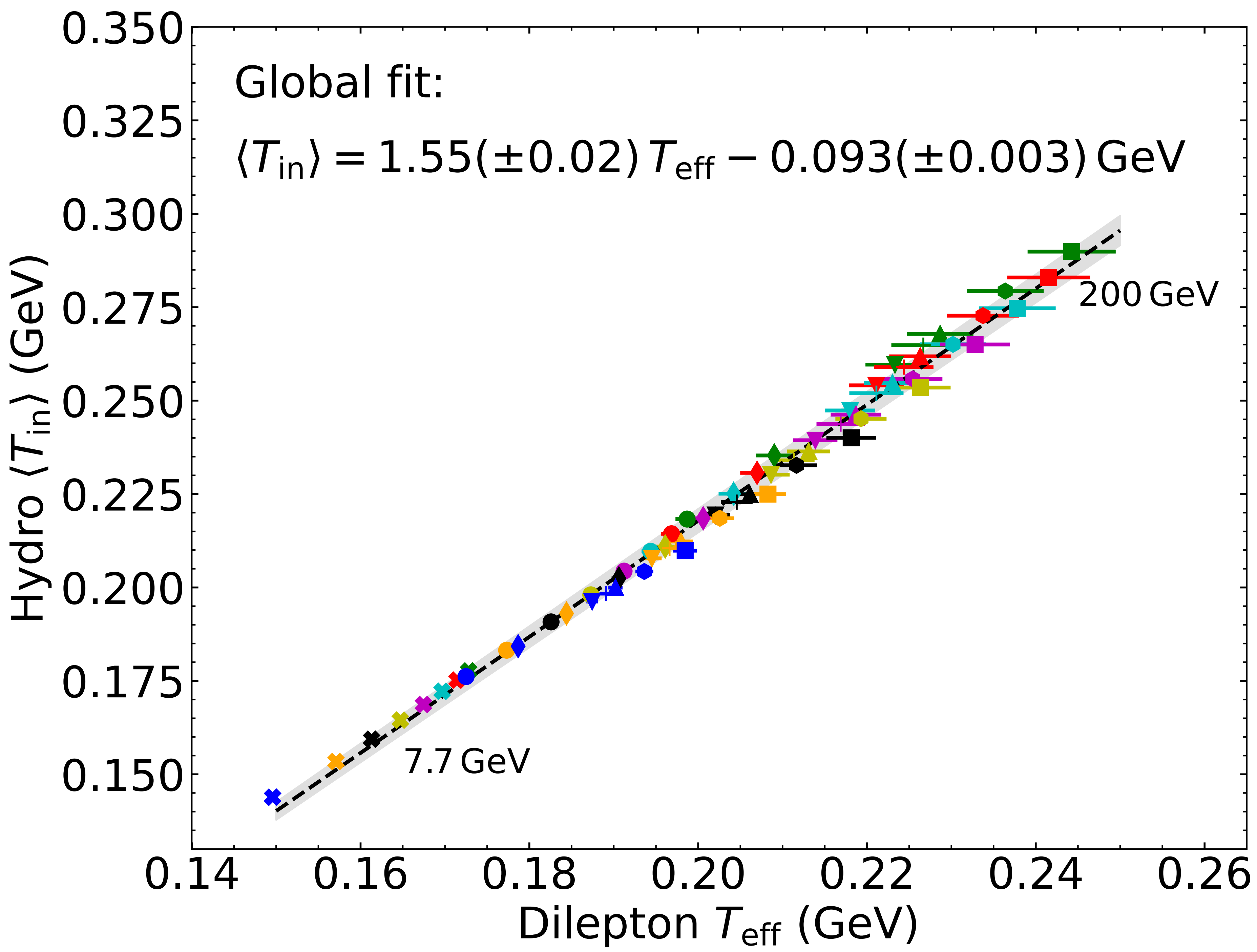


$$\boxed{\frac{dR}{dM} \propto (MT)^{3/2} e^{-M/T}}$$

https://github.com/LipeiDu/DileptonEmission

J. Churchill, LD, C. Gale, G. Jackson & S. Jeon, PRC 109, 044915 (2024), PRL 132, 172301 (2024)

- Combining all energies and centralities, a strong correlation is observed between the initial hydro temperature and the effective temperature extracted from the dilepton spectra
- Measure the temperature of the evolving QCD fireball in a way that is unaffected by dynamical distortions

Kajantie and Miettinen, Z. Phys. C 9, 341 (1981); Hwa and Kajantie, PRD 32, 1109 (1985); Rapp and van Hees, PLB 753, 586 (2016);

# OPPORTUNITIES

- Unique Physics:
    - Region to search for the QCD critical point
    - QCD at high baryon density (especially, multi-messenger at $\mu_B \neq 0$)
    - Connection to neutron star physics
    - Stronger constraints from rapidity-dependent measurements
        - EOS, baryon stopping, energy deposition, etc.
- Urgent Questions:
    - Constraining the longitudinal flow (both initial and final)
    - Transport coefficients of charges
    - Quantitative studies with limited rapidity data

# THANK YOU FOR YOUR ATTENTION!

# A THEORY OVERVIEW

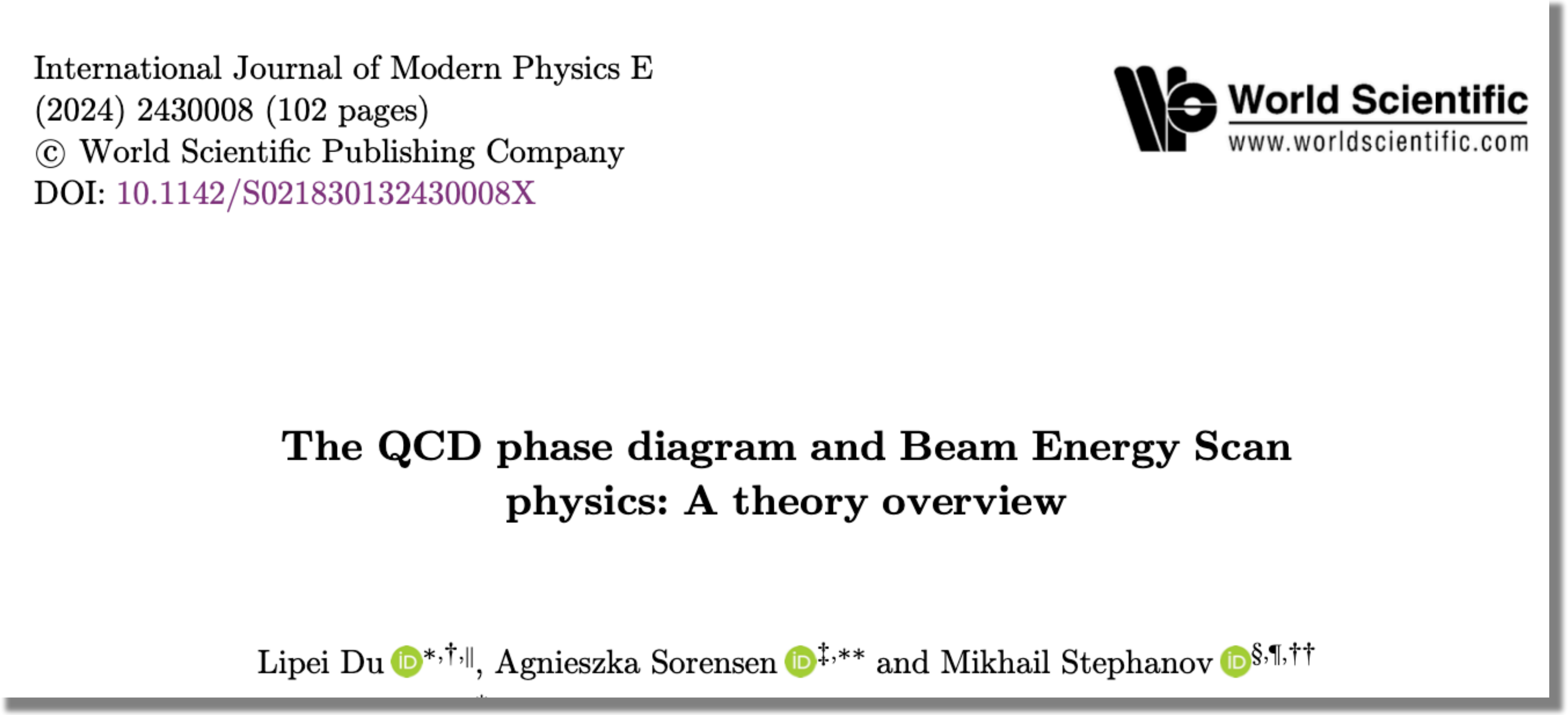

International Journal of Modern Physics E
(2024) 2430008 (102 pages)

DOI: 10.1142/S021830132430008X



**The QCD phase diagram and Beam Energy Scan physics: A theory overview**

Lipei Du[*,†,∥], Agnieszka Sorensen[‡,**] and Mikhail Stephanov[§,¶,††]

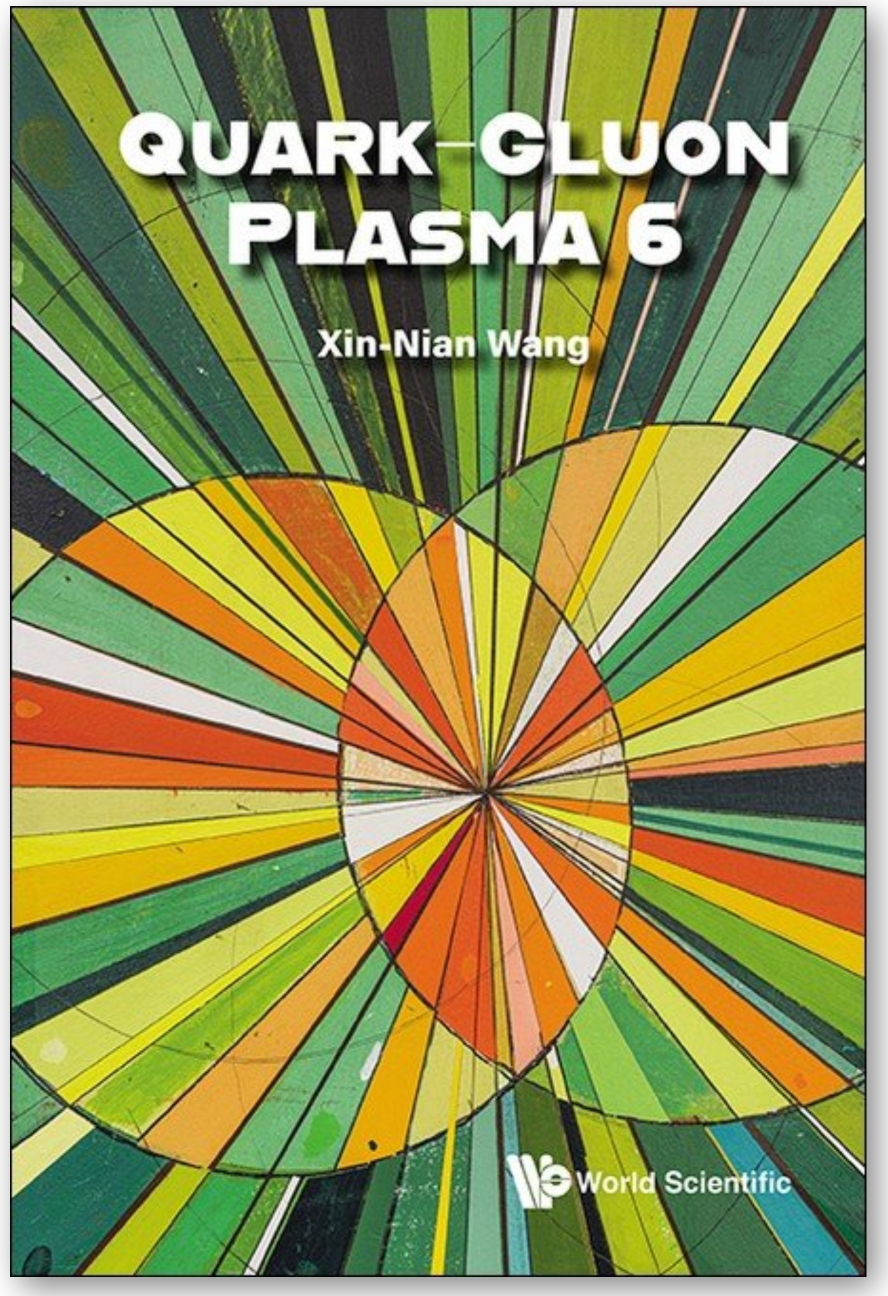


L. Du, A. Sorensen, and M. Stephanov, Int.J.Mod.Phys.E 33 (2024) 07, 2430008 (a contribution to Quark-Gluon Plasma 6)

# MULTI-STAGE MODEL

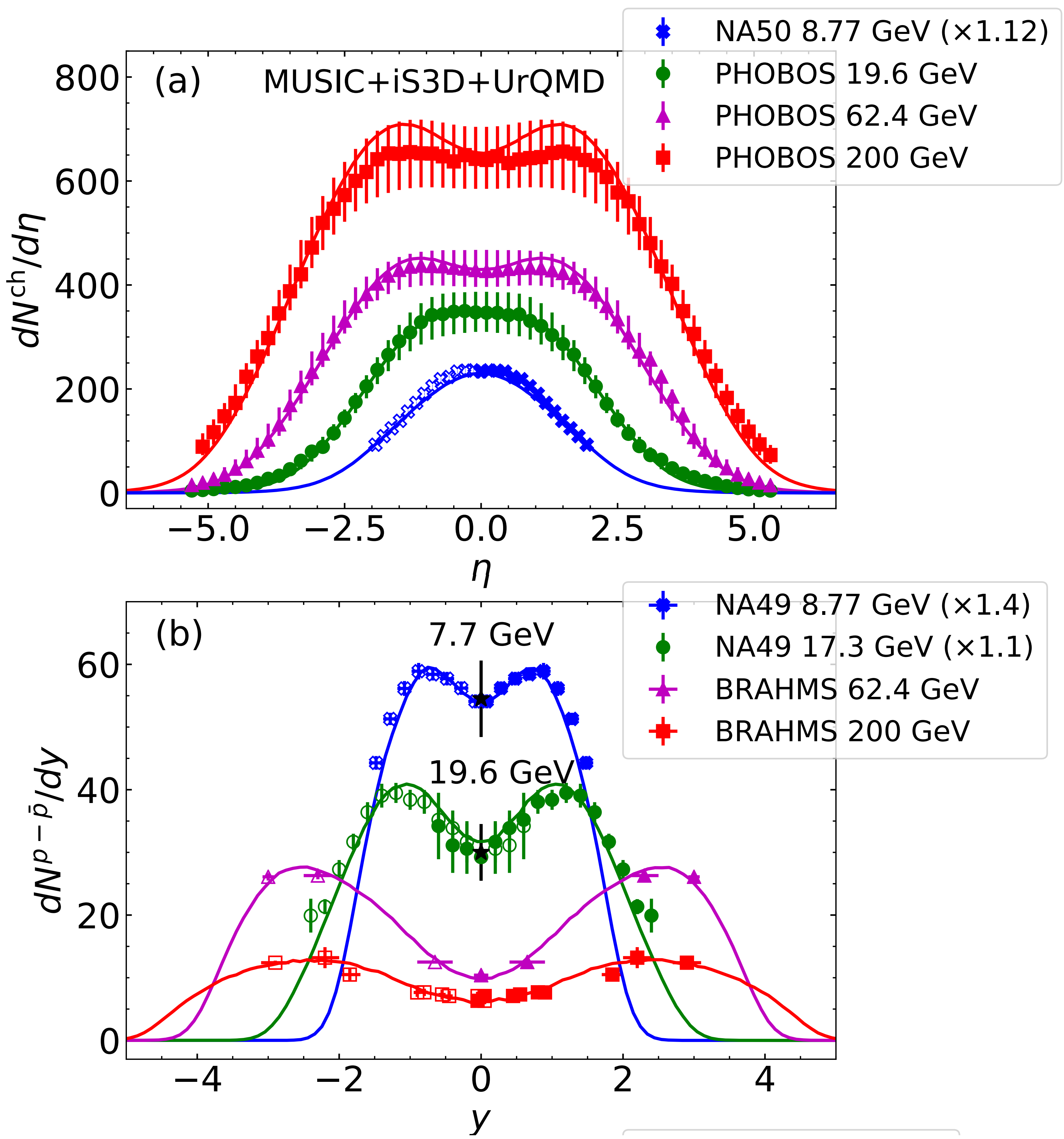


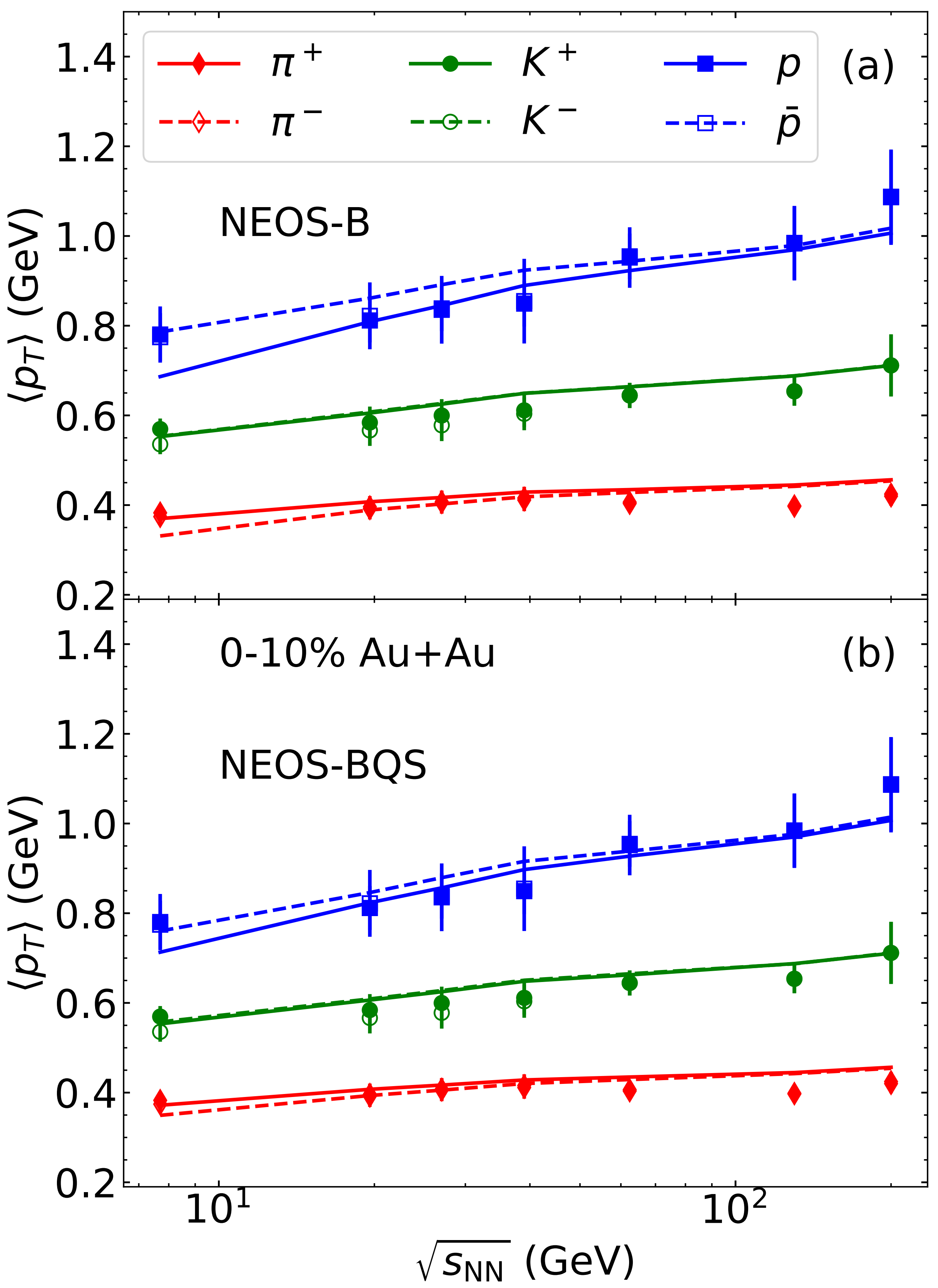


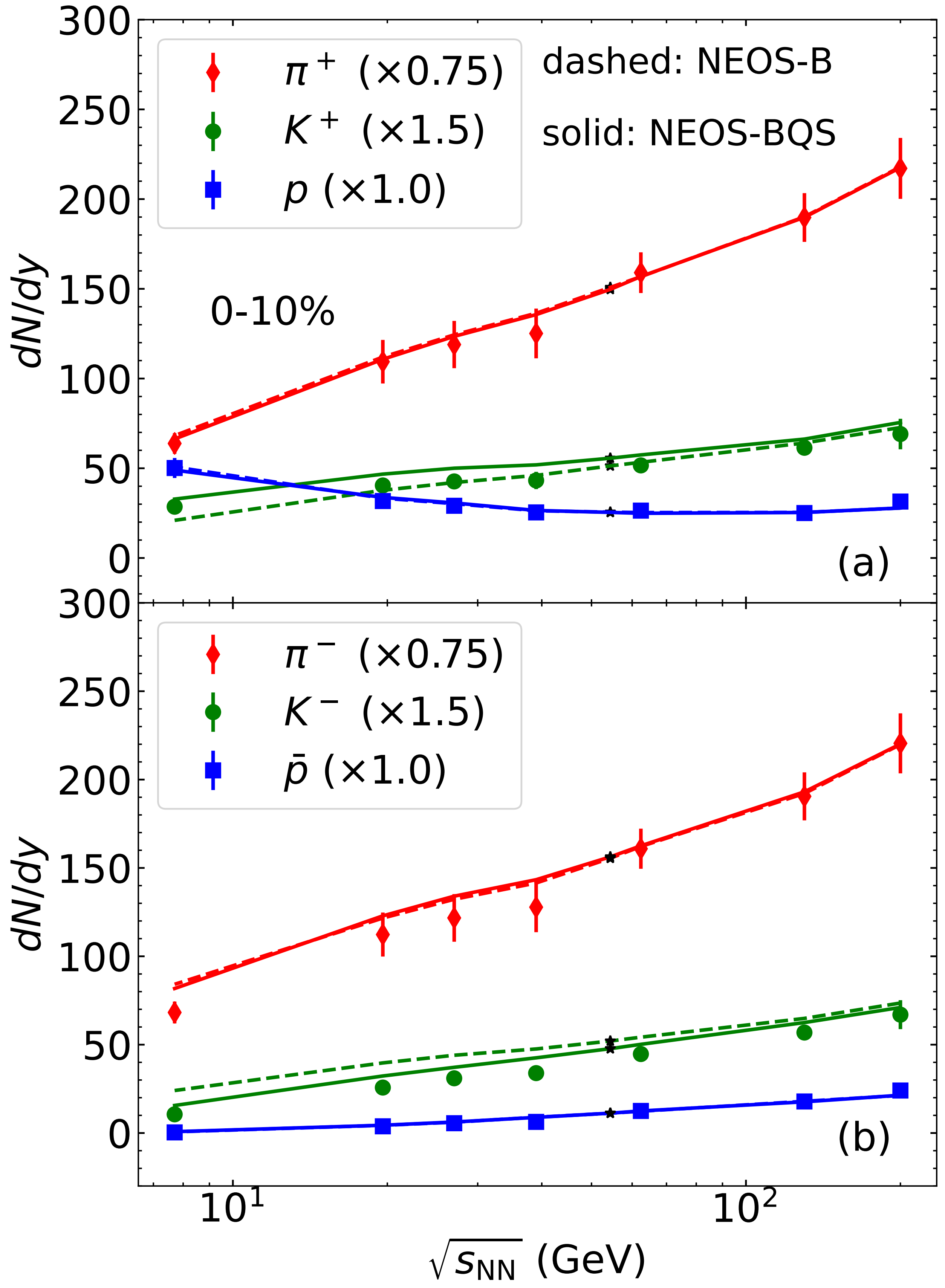


**LD**, C. Shen, S. Jeon & C. Gale, PRC 108 (2023) L041901; **LD**, H. Gao, S. Jeon & C. Gale, PRC 109, 014907 (2024); **LD**, PRC 110 (2024) 1, 014904

- Multi-stage description of Au+Au collisions at $\sqrt{s_{\mathrm{NN}}} = 7.7, 19.6, 27, 39, 54.4, 62.4, 130, 200$ GeV

# DIRECTED FLOW $v_1(y)$ OF PROTONS

reaction plane

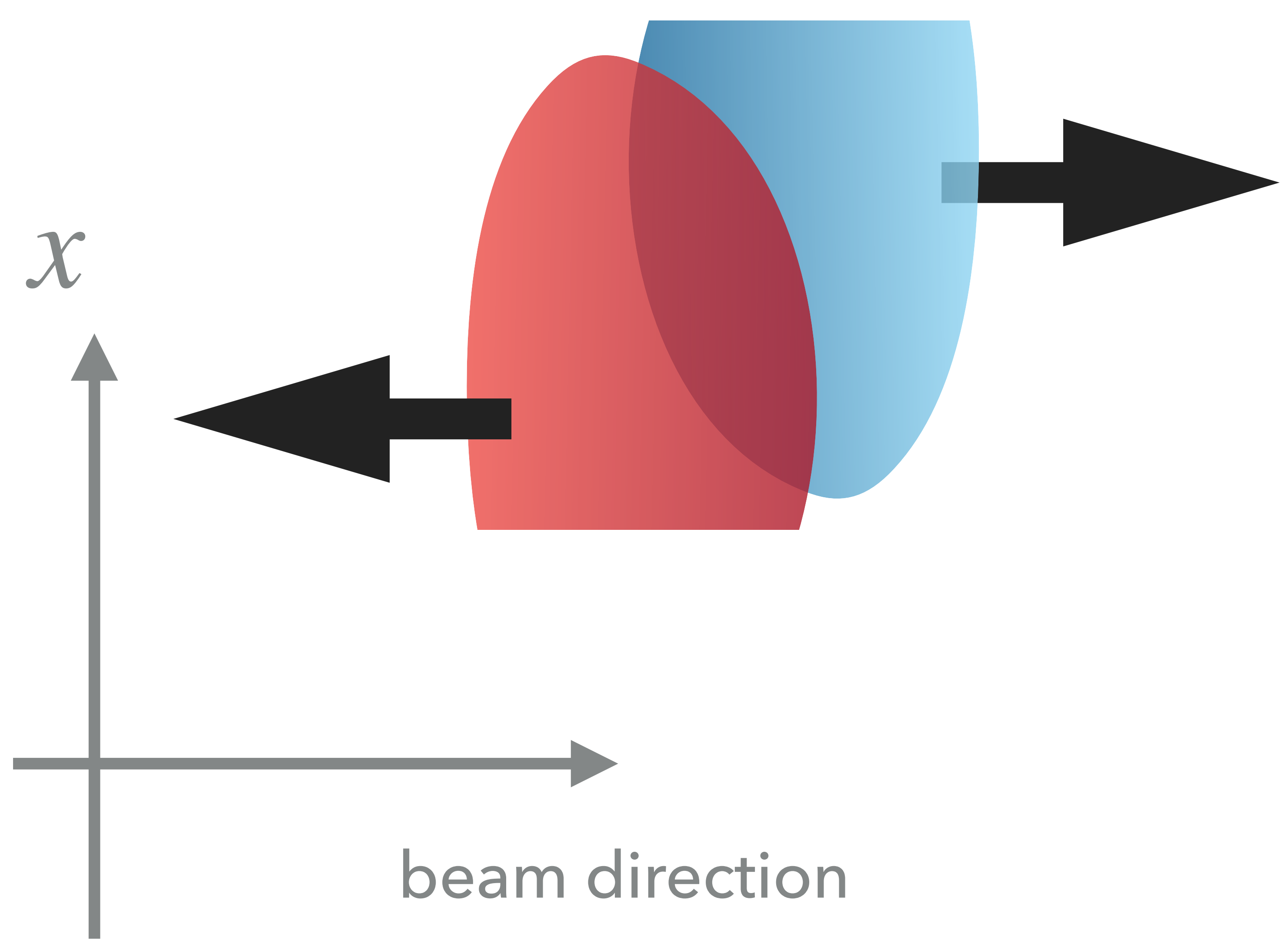


beam direction

transverse plane

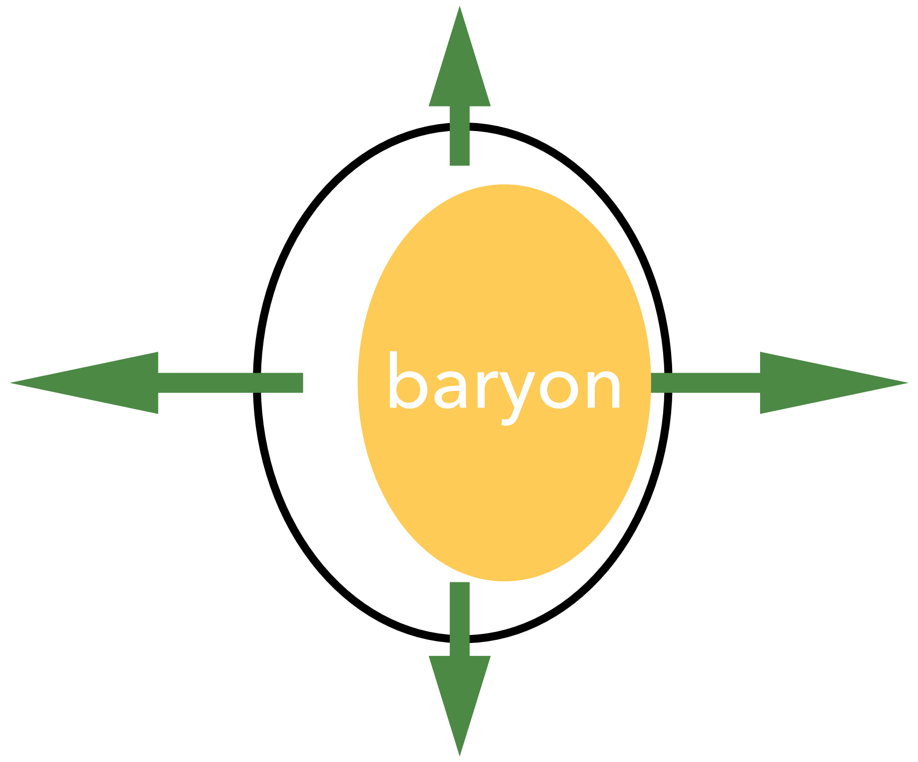


non-zero $v_1$ for baryons

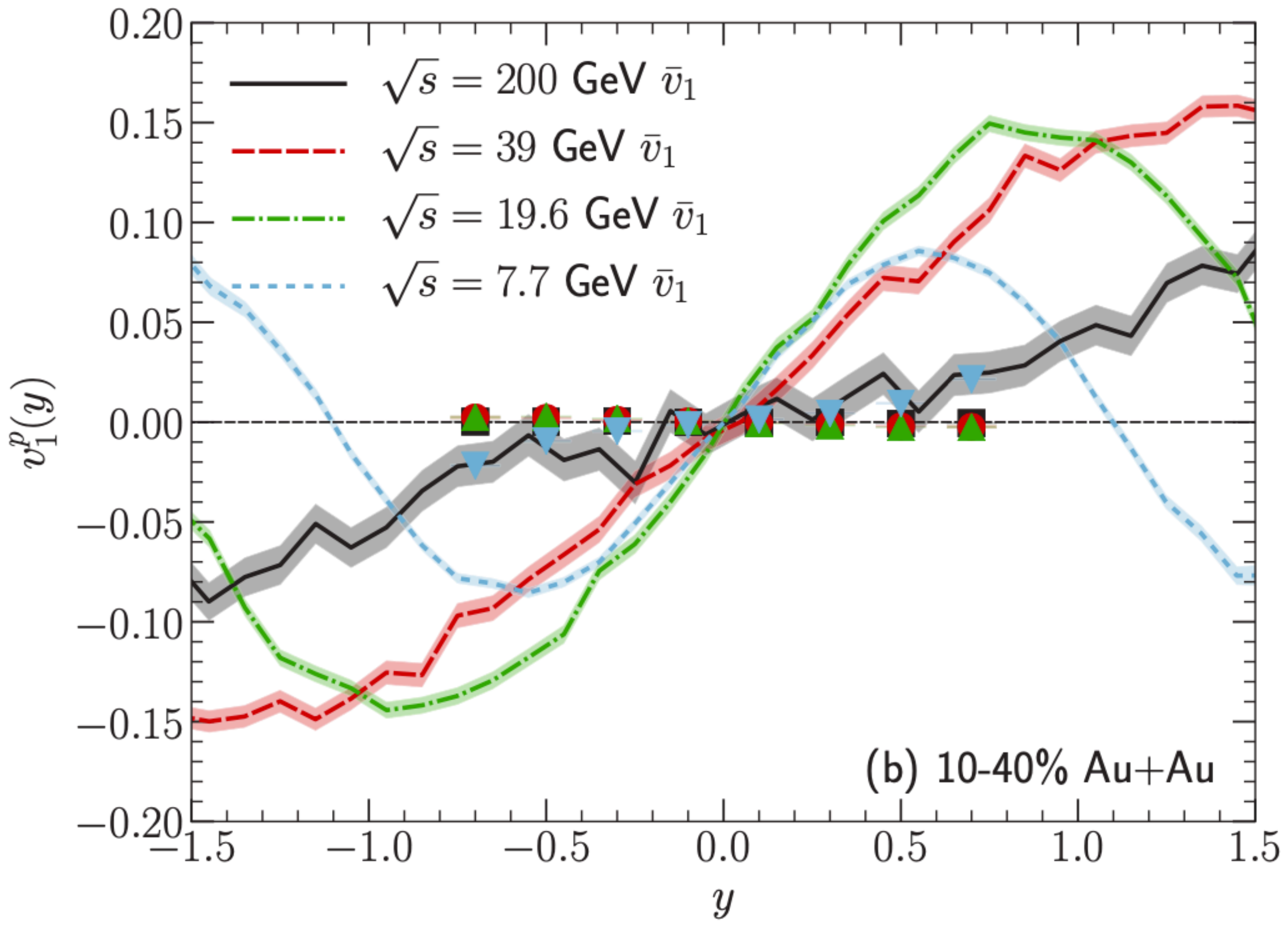


Shen and Alzhrani, PRC102, 014909 (2020)

- $v_1(y)$ of baryons is strongly driven by the asymmetric distribution of baryon density with respect to beam axis + transverse expansion;
- The widely used baryon-stopping picture results in $v_1(y)$ significantly overshooting the experimental measurements for protons at all beam energies.

# NEW PARAMETRIC BARYON INITIAL CONDITION

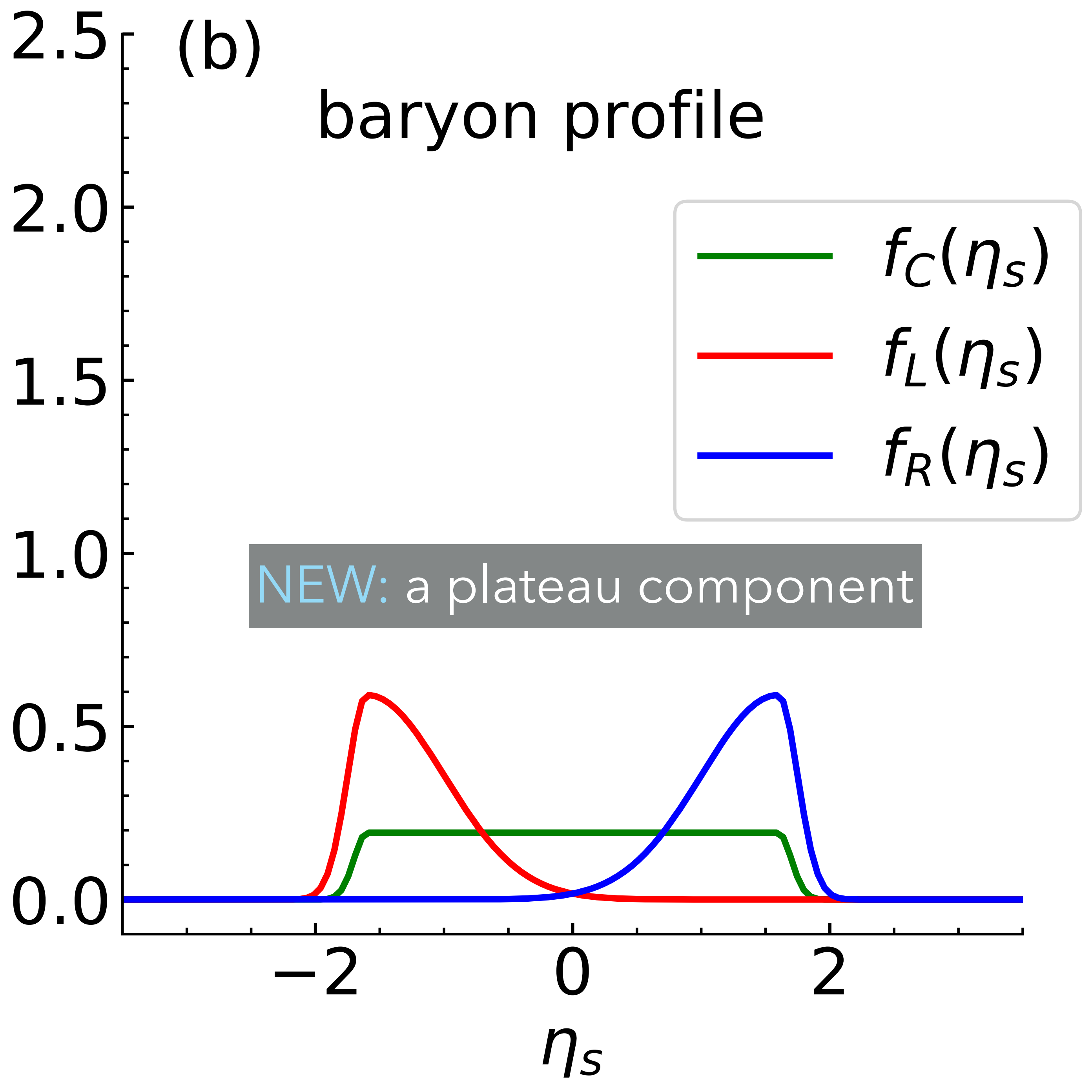


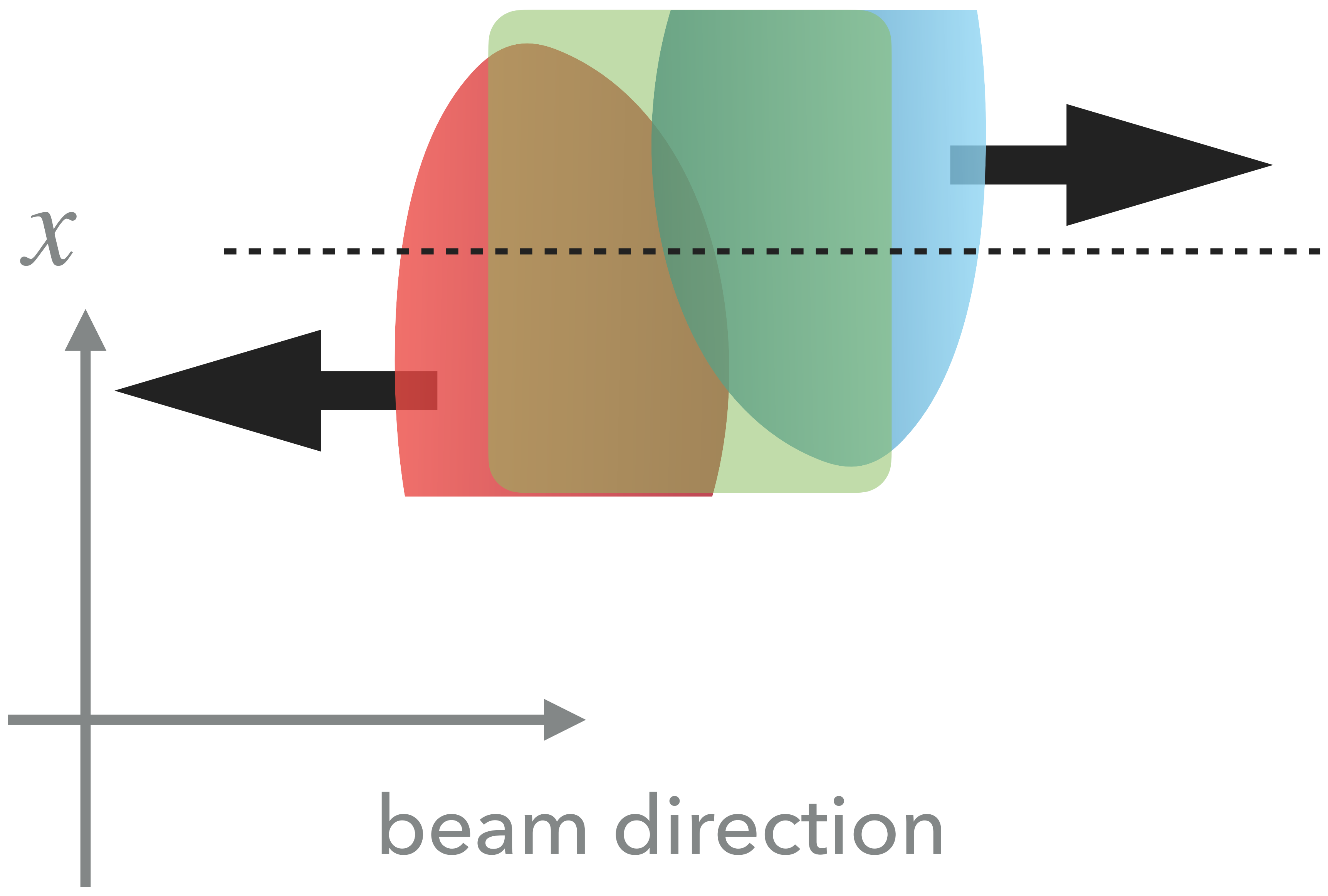


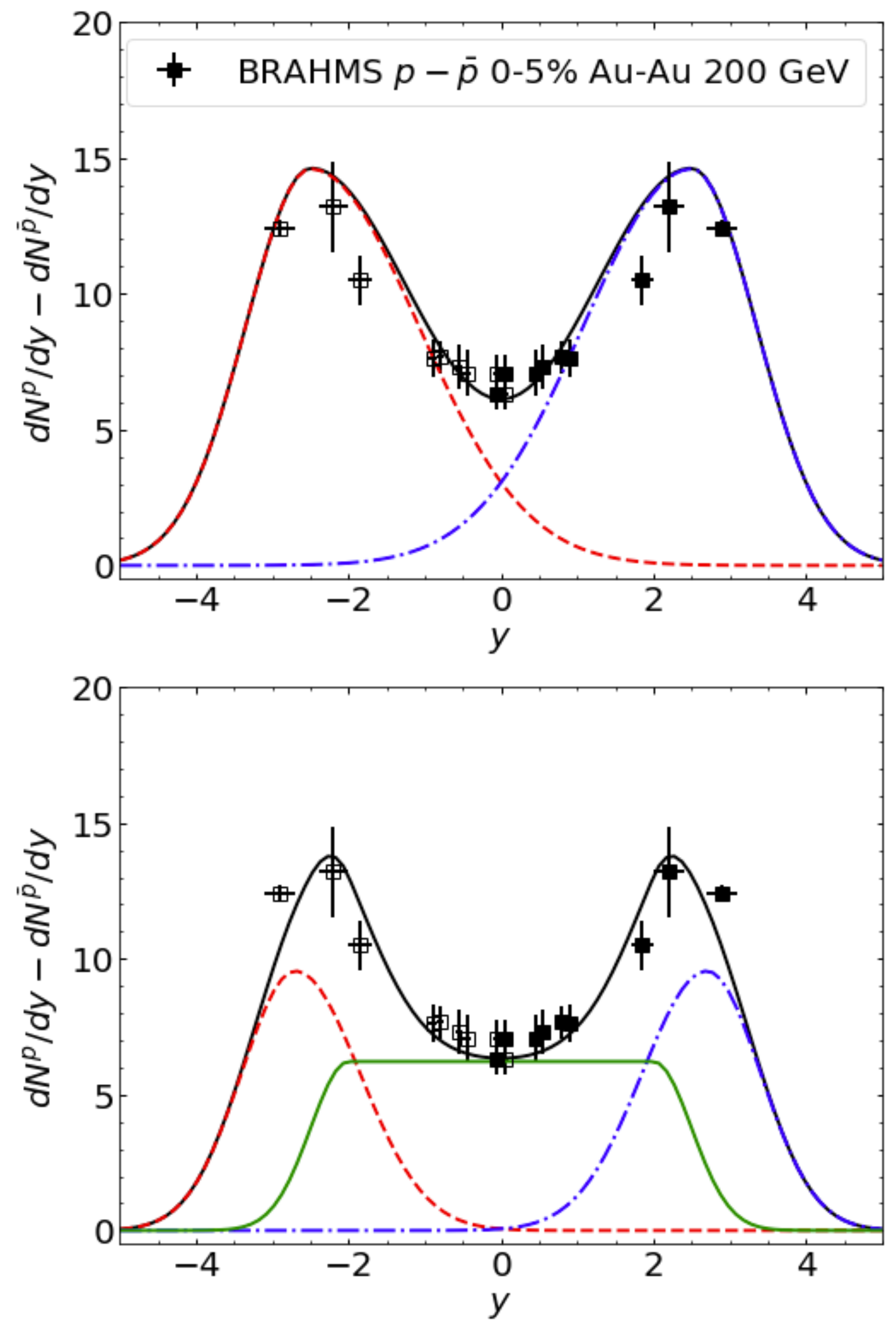


LD, C. Shen, S. Jeon & C. Gale, PRC 108 (2023) L041901

Only for illustration

- To explain the rapidity distributions of net proton yields and baryons' directed flows simultaneously, a plateau component is favored

String junction: Kharzeev, PLB 378, 238 (1996); Sjostrand & Skands, NPB 659, 243 (2003)

# DIRECTED FLOW OF BARYONS AT 200 AND 62.4 GEV

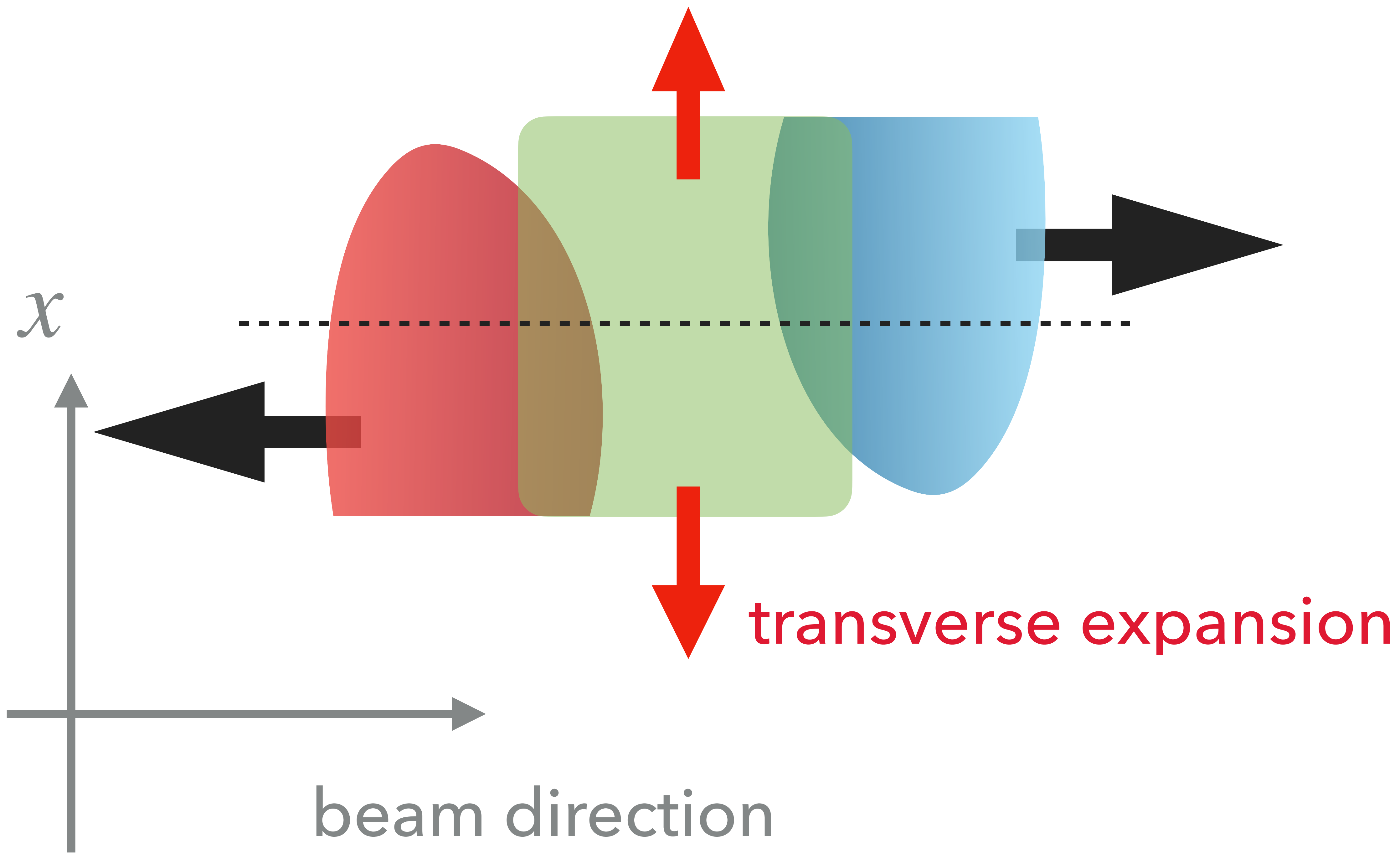


LD, C. Shen, S. Jeon & C. Gale, PRC 108 (2023) L041901

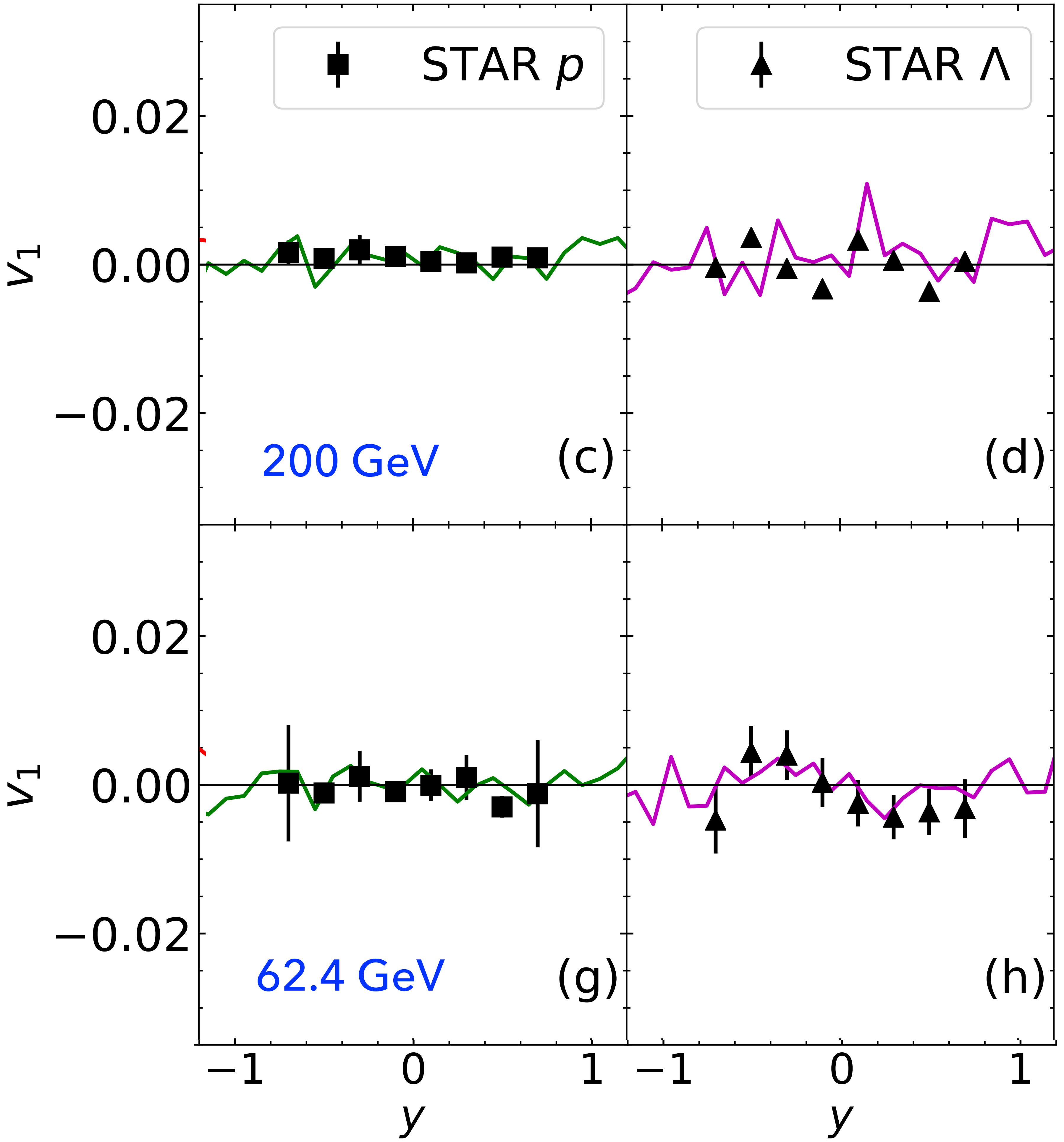


- At high beam energies with large beam rapidities, the plateau dominates around mid-rapidity and strongly reduces baryons' $v_1(y)$.

Data: STAR, PRL 112, 162301 (2014); PRL 120, 062301 (2018)

# DIRECTED FLOW OF BARYONS AT 19.6 GEV

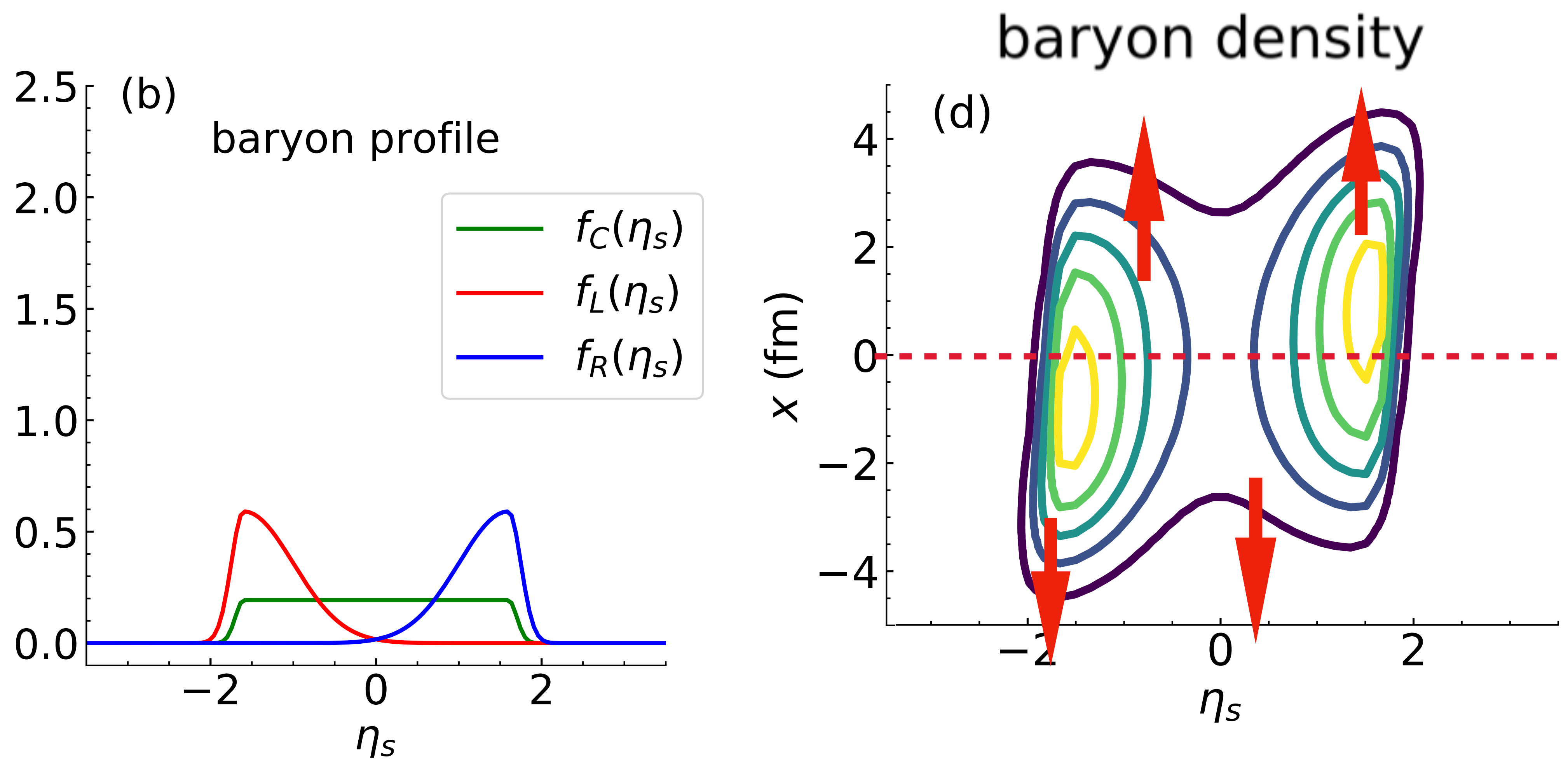


Initial baryon distributions in the reaction plane for
10-40% Au+Au@19.6 GeV

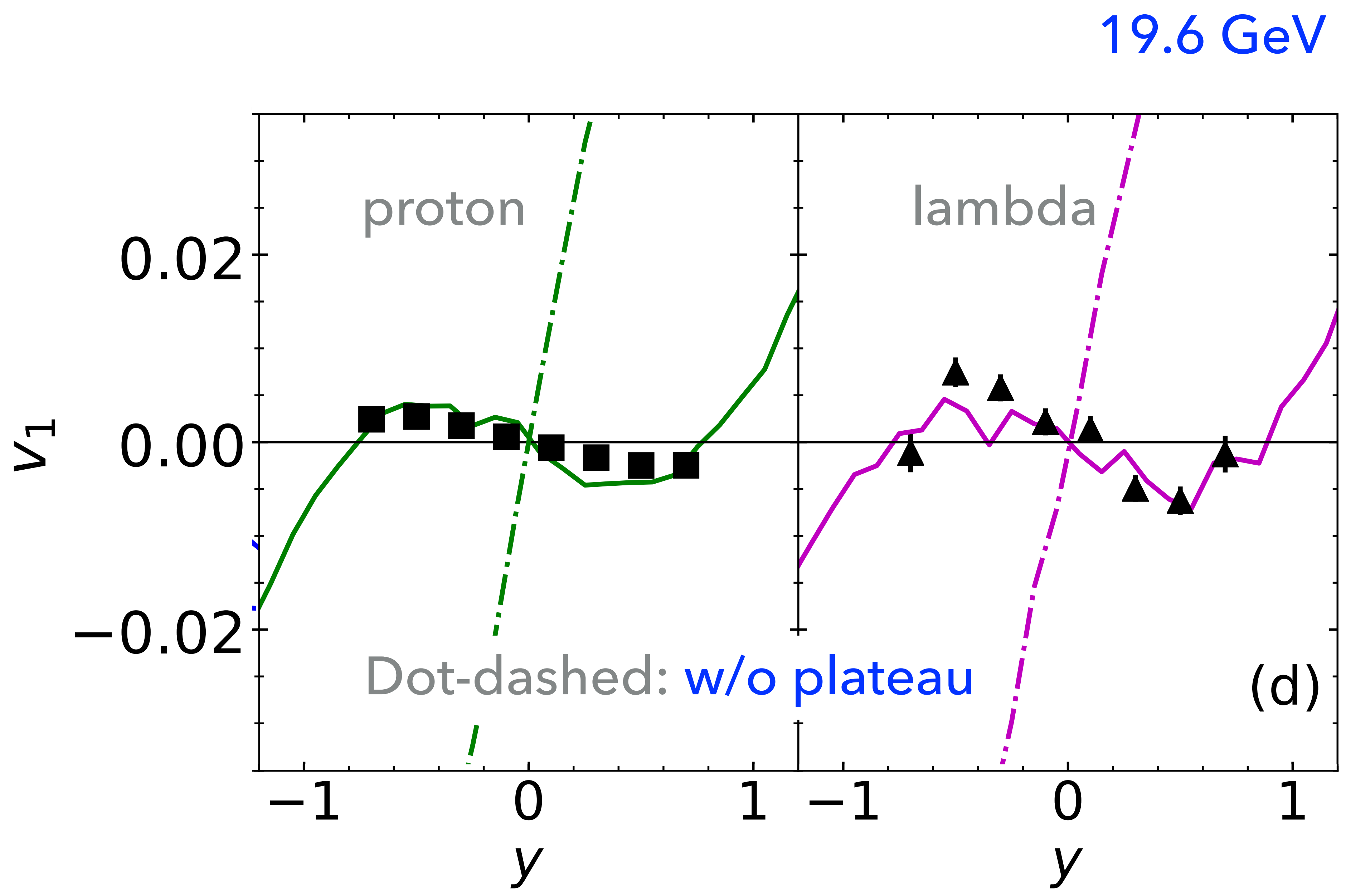


LD, C. Shen, S. Jeon & C. Gale, PRC 108 (2023) L041901

- Transverse expansion + asymmetric distribution of baryon density along x $\Longrightarrow$ double sign change in the slope of $v_1(y)$ for baryons at 19.6 GeV, and positive slope at 7.7 GeV
- The sign change of $dv_1(y)/dy\,|_{y=0}$ is naturally reproduced without a 1st-order phase transition.

# DIRECTED FLOW OF BARYONS AT 7.7 GEV

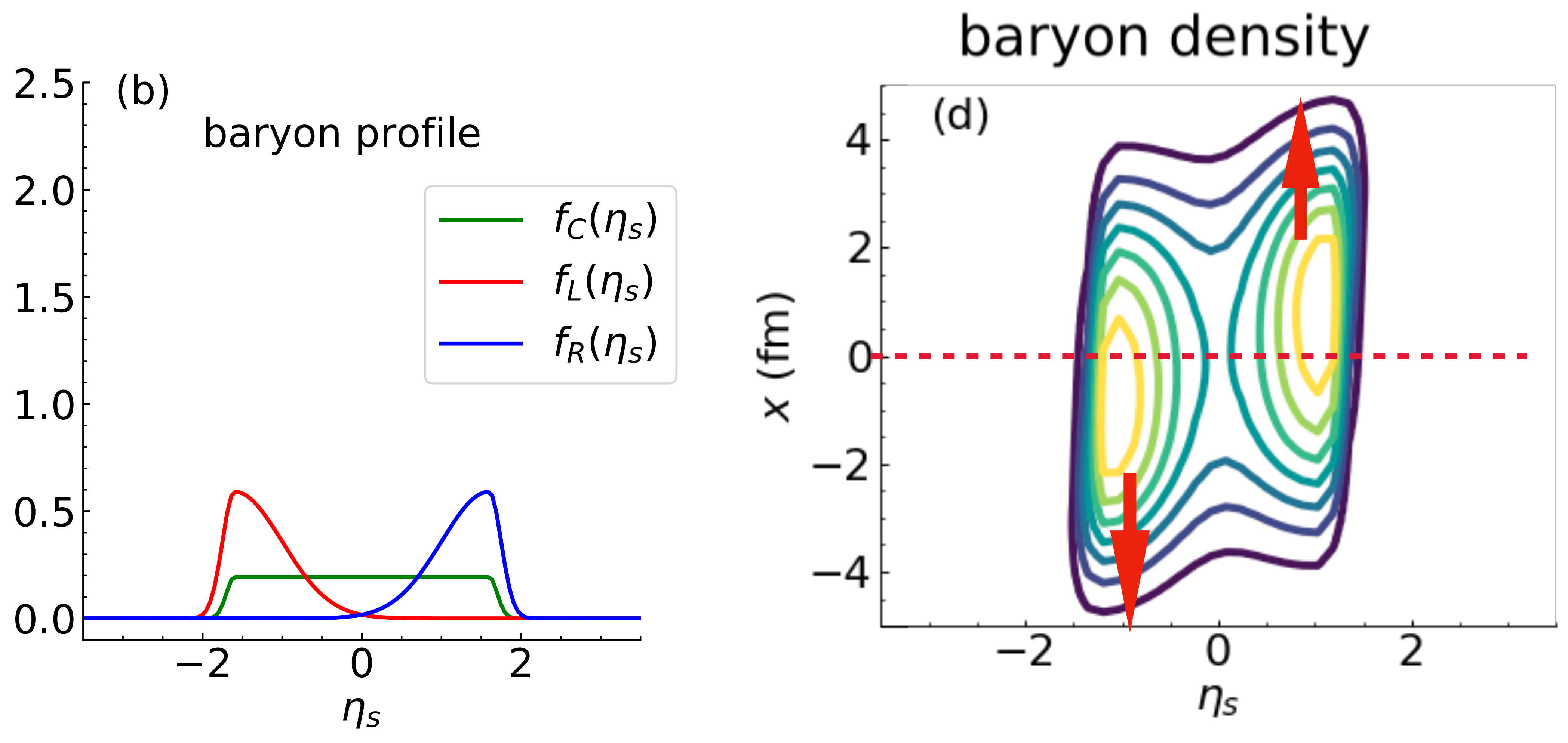


Initial baryon distributions in the reaction plane for 10-40% Au+Au@7.7 GeV

7.7 GeV

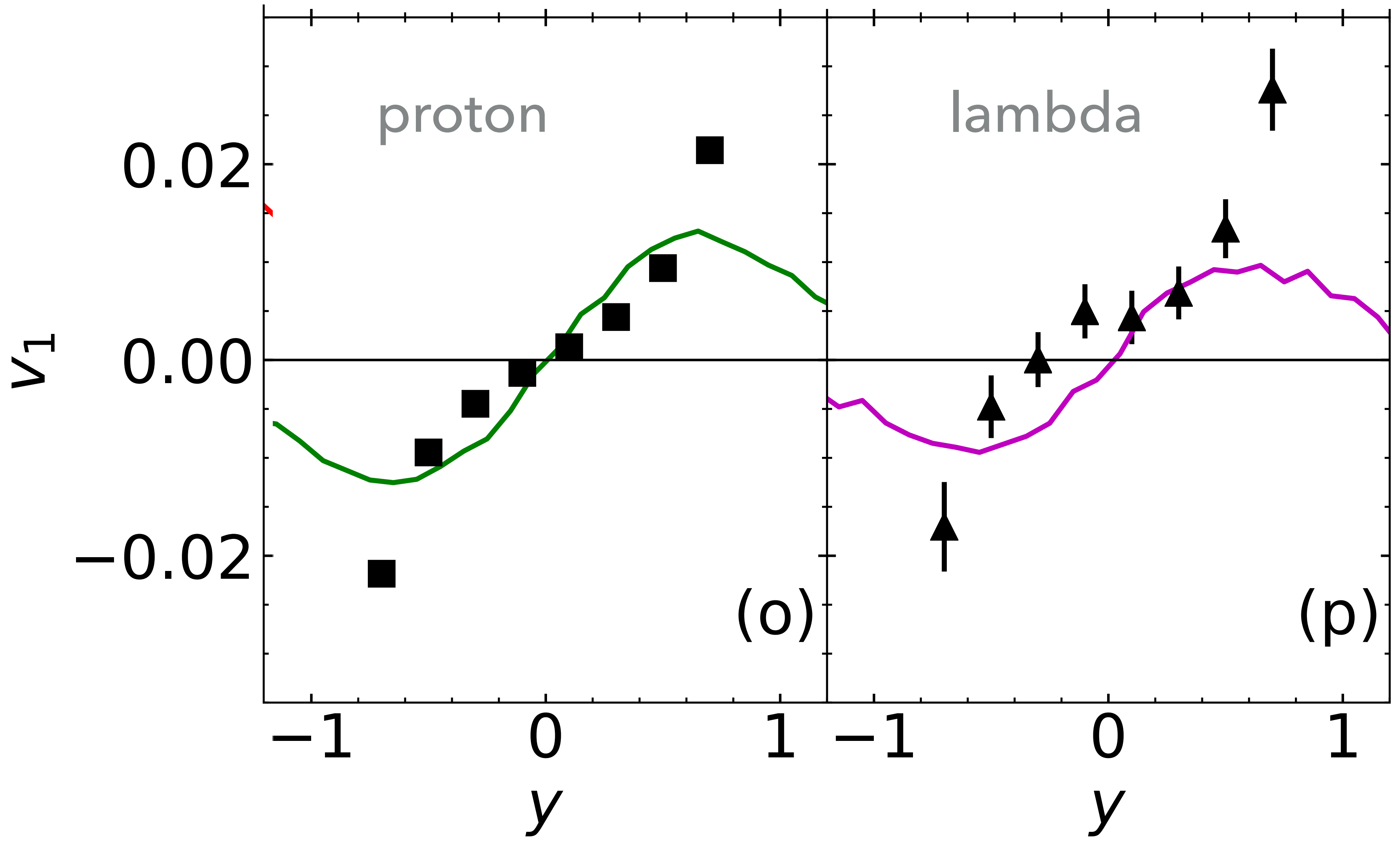


LD, C. Shen, S. Jeon & C. Gale, PRC 108 (2023) L041901

- Transverse expansion + asymmetric distribution of baryon density along x $\Longrightarrow$ double sign change in the slope of $v_1(y)$ for baryons at 19.6 GeV, and positive slope at 7.7 GeV
- The sign change of $dv_1(y)/dy\,|_{y=0}$ is naturally reproduced without a 1st-order phase transition.

# PROBING EOS AT FINITE CHEMICAL POTENTIALS

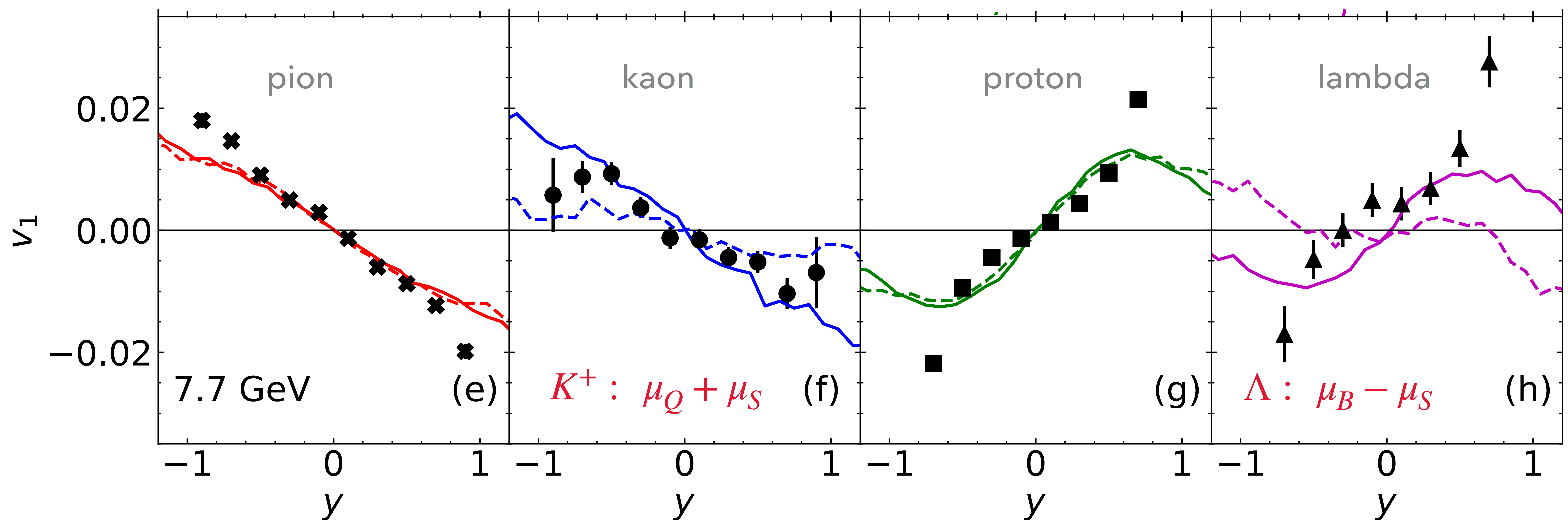


Solid: NEOS-B

Dashed: NEOS-BQS

NEOS: Monnai et al, PRC 100, 024907 (2019)

- Two limits of EoS: NEOS-B, $\mu_S = \mu_Q = 0$ and NEOS-BQS, $n_S = 0, n_Q = 0.4 n_B$ (2D projection of a 4D EOS)
- Local strangeness neutrality suppresses the $v_1(y)$ of $K^+$ and $\Lambda$ around midrapidity, and even alters the sign of $\Lambda$'s $v_1(y)$ beyond $|y| \gtrsim 0.6$
- The $v_1(y)$ of identified particles can be used to probe EoS at finite chemical potentials.

LD, C. Shen, S. Jeon & C. Gale, PRC 108 (2023) L041901

# RAPIDITY AND $\mu_B$ DEPENDENCE

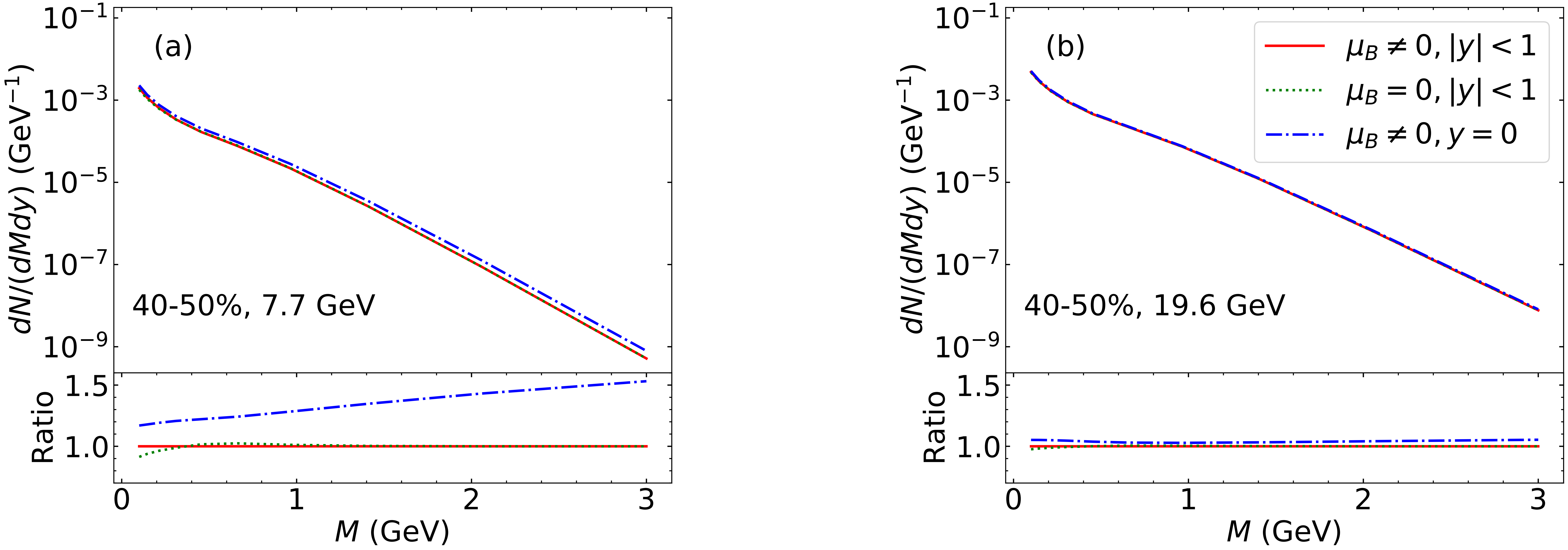


J. Churchill, LD, C. Gale, G. Jackson & S. Jeon, PRC 109, 044915 (2024), PRL 132, 172301 (2024); L. Du, Phys.Lett.B 861 (2025) 139270

- $\mu_B$-dependence is not significant for 7.7 GeV and higher beam energies
- At 7.7 GeV, a strong boost-non-invariant effect is observed